ECN

Registered

Design for Reliable power performance (D4REL)

Final report

ECN-E--17-051 - September 2017

Design for Reliable power performance (D4REL)

Author(s)

S. Kanev
U. Shipurkar
D. Baldachino
H. Ozdemir
J. Peeringa
Y. Gunes

In co-operation with

Acknowledgement

Het project is uitgevoerd met subsidie van het Ministerie van Economische Zaken, Subsidieregeling energie en innovatie (SEI), Topsector Energie uitgevoerd door Rijksdienst voor Ondernemend Nederland.

The authors would like to thank TKI Wind op Zee for funding this project.

Table of contents

Summary

Design for Reliable Power Performance (D4REL) is an R&D project aiming at developing innovative technology & tools for reducing uncertainty in both the design and operation of offshore wind farms, with the goal of achieving substantial reduction of 6.4% of the cost of energy (CoE).

This project aims to develop new technology and tools for the reduction of uncertainty in both the design phase of wind farms and its operational life. By lowering design and operational uncertainty, the designs can be made less conservative and operation can be optimised.

Improving the predictability of the performance of large offshore wind farms implies the development of tools and methods that assist the designer and operator/developer in achieving a reliable asset management of the offshore wind power plant. Key in this target is the optimal operation of the wind turbine and the ability of the wind turbines to take the autonomous decisions on optimal operation.

This project has developed a wide range of novel technologies that increase the reliability of the wind turbine and reduce the performance uncertainties. These are:

- Availability improvement in electrical generator systems by means of:
  - Modular concepts in power electronic converters: these are shown to reduce the failure rates and increase the availability of generator systems
  - Converter topologies: different three-level topologies, the 3L-ANPC and the 3L-T2C show the highest lifetimes
  - Dynamic thermal management: control of junction temperature is shown to achieve a significant reduction of damage in the power semiconductor.
- Improved knowledge and design capability (modelling) enabling the development of the next generation of larger and lighter offshore wind turbine blades:
  - Vortex generators: these are blade add-ons that increase the power yield significantly, and enable the use of thicker airfoil profiles
  - Thick trailing edges: they enable the use of long slender rotors equipped with thicker blades, enabling the design of larger rotors with smaller solidity.
  - Modelling of thick airfoils: Improved lift and drag prediction enables more reliable design (low uncertainty) design of the next generation thicker blades
- Probabilistic support structure design:
  - By taking the uncertainties in the support structure design explicitly (instead of indirect by using partial safety factors), design of support structure with a lower mass is shown viable.
- Wind turbine modelling and control:

- System identification: improved nonlinear system identification methods are developed, including uncertainty quantification, to enable the use of advance adaptive control algorithms
- An adaptive control algorithm is developed, with its parameters being adapted online during operation based on the measured/identified support structure parameters. It reduces the loads on the support structure in the presence of uncertainty in the support structure frequency due to design uncertainties (manufacturing, installation, soil) and operational uncertainties (scour, formation of marine sand dunes and biofouling). It also enables significant material cost reduction in the tower.
- Condition based control: the controller is adjusted to reduce the loads on a part with a deteriorating condition, with the aim of delaying failure and increasing the total energy produced until the moment of failure. This reduces downtime substantially.

These results have been disseminated over various journals, conferences and workshops.

The impact of the project is estimated as:

- AEP improvement: approximately is 2.5% , based on 2% increase in AEP due to vortex generators and approximately 0.5% increase in availability.
- 9.7% reduction of the support structure CAPEX. The share of the support structure cost on the total required CAPEX of an offshore wind farm is approximately 20 – 25%, for water depth of approximately 30 – 35 m. This would then result in a total reduction of CAPEX of approximately 2%.

This boils down to 3.6% cost reduction of the LCoE.

1. Project overview

1.1 Project information

A table containing main project information is given in Table 1.

Project title	Design for Reliable power performance (D4REL)
Project number	TKIW02007
Coordinator	Stoyan Kanev (ECN)
Duration	1 October 2013 – 30 September 2017

Table 1 Summary of main project information

The project partners are:

- **ECN**: project coordinator, Applied research institute
- **TU-Delft**: Fundamental research institute
- **Siemens**: Wind turbine manufacturer
- **Van Oord**: Engineering, Procurement and Construction contractor
- **IHC Hydrohammer**: Manufacturer of hydraulic piling hammers
- **Eneco**: Utility

As such a strong consortium was built consisting of the whole technology chain from fundamental research to industrial application.

The project was divided into 4 work packages (Figure 1). These are:

WP1: Electrical generator systems for reliability
Aim: improving the availability of electrical generator systems by using modular conversion system concepts that are fault tolerant, re-configurable and self-healing.

WP2: Next Generation of Robust Offshore Blades
Aim: generating the knowledge and design capability that enables the development of the next generation of larger and lighter offshore wind turbine blades that do not rely on failure prone features and thereby lower the cost of energy.

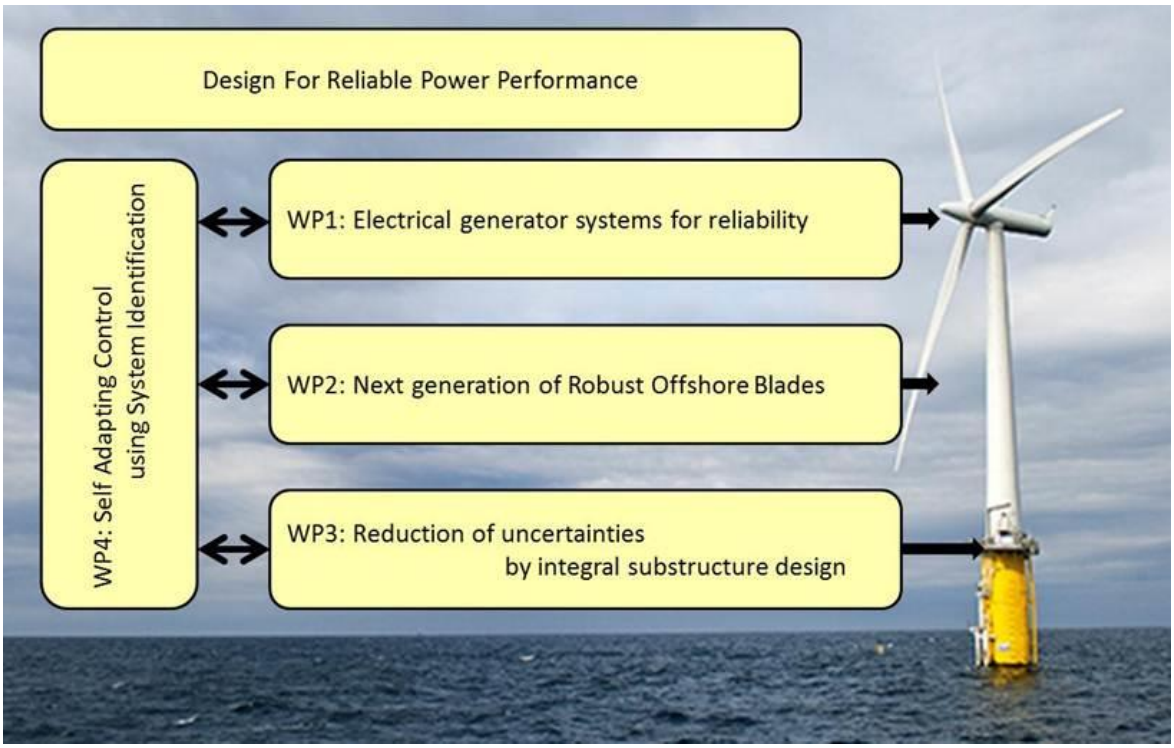

Figure 1 Project structure

WP3: Reduction of uncertainties by integral substructure design
Aim: realizing cost reduction in the support structure of offshore wind turbines while keeping a sound, safe and reliable design by using integral probabilistic structural design techniques; developing self-adaptive control algorithms dealing with constantly changing environmental conditions (e.g. water depth changes due to tides and/or scour, ice formation, etc.).

WP4: Self adapting control using system identification for robust control
Aim: Improve the availability of offshore wind turbines by developing, (a) innovative adaptive controllers that optimize their performance using estimation of time-varying turbine parameters from system identification, and (b) condition based control that delay approaching failures by operating the turbine at reduced loading on parts with deteriorated condition.

1.2 Objectives

D4REL is a R&D project aiming at developing innovative technology & tools for reducing uncertainty in both the design and operation of offshore wind farms, with the final goal of 6.4% LCoE reduction.

Limiting the design uncertainty makes it possible to reassess and reduce the safety factors which are used in the design of wind turbines to account for the modelling uncertainty in the design process. More accurate modelling allows for lower safety factors, which in turn makes it possible to achieve less conservative (and, hence, cheaper) turbine design.

The operational uncertainty will be reduced by using fault tolerant and condition-based control methods. Fault tolerant control aims at accommodating simple, non-critical failures in the wind turbine by reconfiguring the control algorithm to prevent unnecessary shutdowns (missed production). Condition-based control, on the other hand, employs health monitoring techniques

that indicates an approaching critical component failure, and adapts the control algorithm to reduce the load of that component and delay/avoid failure. Hence, the fault tolerant and condition-based control methods will lead to less unplanned maintenance and higher supply certainty.

Improving the predictability of the performance of large offshore wind farms implies the development of tools and methods that assist the designer and operator/developer in achieving a reliable asset management of the offshore wind power plant. Key in this target is the optimal operation of the wind turbine and the ability of the wind turbines to take the autonomous decisions on optimal operation. Aiming for a more reliable wind turbine with low performance uncertainties, the main objectives defined in this project are as follows:

- Improving the availability of electrical generator systems by using modular conversion system concepts that are fault tolerant, re-configurable and self-healing;
- generating the knowledge and design capability that enables the development of the next generation of larger and lighter offshore wind turbine blades that do not rely on failure prone features and thereby lower the cost of energy;
- realizing cost reduction in the support structure of offshore wind turbines while keeping a sound, safe and reliable design by using integral probabilistic structural design techniques;
- developing self-adaptive control algorithms dealing with constantly changing environmental conditions (e.g. water depth changes due to tides and/or scour, ice formation, etc.);
- substituting unplanned with planned maintenance by bridging the gap between existing condition monitoring and fault tolerant control schemes.

1.3 Approach

To realize the goals of the project, fundamental and industrial research activities are conducted. This project focuses mainly on fundamental research, carried out by PhD students at the TU-Delft, and by researchers at ECN. Siemens is involved in applied research and wind tunnel experiments primarily related to the improved modelling of blade add-ons (vortex generators) and thick trailing edge airfoils (WP2). Van Oord, and to a lesser extend IHC Hydrohammer, are also involved as technical advisors, providing expertise in design and installation of foundations (topic of WP3). Below, the approach per work package is outlined.

1.3.1 WP1 Electrical generator systems for reliability (TU-Delft)

Background: Generator systems (including generator and power electronic converter) of wind turbines fail far too often, especially offshore, which leads to significant down time and repair cost. Large R&D programmes have been executed to analyse the failure mechanisms of offshore wind turbines. These programmes target blade monitoring, support structure, drive train, etc. Although there has been significant research in this area, in practice, the electrical systems are relatively problematic. This work package aims at significantly increasing the turbine availability using fault tolerance in the electrical system of the turbine. An example is to increase the number of phases. Generators normally have three phases, consisting of strings of parallel coils. Converters normally have three phases, consisting of parallel modules. If the three phases of the generator would be split into, for example, 4 sets of three phases and the converter would be split into 4 three-phase converters, the system could continue operation at a reduced power level if one of the sets of three phases fails. This could improve the availability and the energy yield without adding additional cost.

Objective: Improve availability by using modular conversion system concepts that are fault tolerant, reconfigurable and self-healing.

This Work package is organised in the following tasks.

Task 1.1: Analysis of failures in generator systems (TU-Delft)
The objective of this task is to be investigate which failures occur so often that it would be wise to change the design to reduce corrective maintenance and hence to increase the availability.
The following research questions have to be answered:

- Which faults play a role in generators and converters?
- What is the probability of these faults?
- For which of these faults does it make sense to make the system fault tolerance?

Earlier studies suggest that it is worthwhile to consider making the system tolerant to failures in the power electronic switches because these components fail rather often and unexpectedly. These studies also suggest that it might not make sense to make a generator system fault tolerant to short circuit faults in the generator because these failures do not occur so often. This task will be carried out by doing a literature study but especially by creating a strong collaboration with the University of Aalborg.

Task 1.2: Fault avoidance (TU-Delft)
Avoiding faults may be more useful than making generator systems fault tolerant. Therefore, it should be investigated if faults can be avoided by using different components or by designing components in a different way. In order to design components in a more reliable way, knowledge of the failure mechanisms is very valuable.
The main research question in this task is:

- Is it possible to design the system in such a way that these failures are avoided, and if yes, how?

The objective of this task is not to study failure mechanisms in detail, but to create an overview of the possibilities for fault avoidance. The reason to do this is to avoid that extensive work on fault tolerance is done on types of failures that could easily be avoided. This task will be carried out in strong collaboration with the University of Aalborg.

Task 1.3: Inventory and analysis of fault tolerance (TU-Delft)
The objective of this task is to make an inventory of forms of redundancy, re-configurability and fault tolerance in the generator system. This includes modular generator systems, multilevel converters and multi-phase systems. Analysis of these systems may result in proposals for new topologies. Fault tolerance in aircraft systems can serve as inspiration, but should not be copied because of the different requirements: in aircraft system, the objective is uninterrupted operation and the cost may be high; in wind turbines the objective is a high availability at low cost.
Based on this initial analysis, some case studies will be selected that will be worked out in detail in the next phase.
The following research questions have to be answered:

- Which forms of redundancy and re-configurability in the generator system are possible?
- Which of these would be most useful of wind energy conversion systems resulting in an increase in availability and reduction of COE?

This task will be carried out by doing a literature study and by doing an initial analysis of the different systems.

Task 1.4: Analysis of the improvement of the availability for case studies (TU-Delft)
The objective of this task is to determine the expected increase in availability for a few case studies in more detail. The availability will be calculated using statistical methods and using

statistical information about failures. The availability of these fault tolerant systems will be compared to the availability of a standard baseline generator system. Mostly, fault tolerant systems consist of higher numbers of components. By definition, adding components (in parallel) leads to a reduction of the mean time between faults. The intention of fault tolerance is to increase the mean time between failures that lead to a system shut down. A careful analysis is necessary to see the effect of the different measures of fault tolerance. Hence, this task will be carried out by modelling the reliability of the selected generator systems. The performance of the fault tolerant generator system under normal and under fault conditions must be analysed: when faults occur, they have to be detected, the control system has to adapt, and the system will operate in a different way.
The following research questions have to be answered.

- How much does the availability increase by using a fault tolerant generator system?
- How can failures be detected (system identification)?
- How can the system be controlled during faults (fault tolerant control)?

This task will be carried out by modelling a simulating the system in a simulation program.

Task 1.5: Writing PhD thesis (TU-Delft)

- The objective of this task is that the PhD student writes a PhD thesis.

1.3.2 WP2 Next Generation of Robust Offshore Blades (ECN, TU-Delft, Siemens)

Background: The quest for robust and higher power output at reduced costs per offshore wind turbine drives the design towards increasingly larger rotor diameters that have positive influence on the usage of the electrical grid (by larger capacity factor) and wind farm power production. To counteract the increased mechanical loading in extreme off-design conditions, these increasingly larger rotors have relatively small solidity. The much slender rotors therefore have to be equipped with thicker rotor blades. The drawback of thicker blade sections is that the use of these rotors are accompanied with relative large uncertainties in performance. This motivates the application of vortex generators (VG) and thick trailing edges (TTE), illustrated in Figure 2. The modelling of rotors with vortex generators and thick trailing edges is a challenge in itself. The entire sector would be greatly assisted when reliable models for the use of vortex generators and thick trailing edges would be available.
In this work package Siemens is collaborating with ECN and TU Delft in the theoretical model development and practical implementation of these flow device models to the RFOIL blade section design code. Siemens will perform extensive wind tunnel measurements together with the TU Delft PhD student and bring in the project the results of previous wind tunnel experiments. The knowledge and experience of the Siemens CFD modelling group will be put to use in this work package.

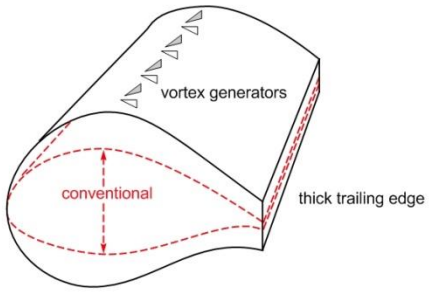

Figure 2 Rotor blade section equipped with vortex generators and thick trailing edge

Objective: The overall objective of work package 'Robust Power Performance' is to generate the knowledge and design capability that enables the development of the next generation of larger and lighter offshore wind turbine blades that do not rely on failure prone features and thereby lower the cost of energy. More specifically, this work package objective is to enable the accurate and reliable simulation of the effects of vortex generators and thick trailing edges on wind turbine performance by extending the existing airfoil design tool RFOIL with models for the effect of vortex generators and thick trailing edges on airfoil aerodynamic performance that are validated against experimental data. From numerical and wind tunnel experiments flow field data will be obtained and analysed to create a vortex generator model that will be implemented in RFOIL. Partners in this work package ECN, Siemens, and TU Delft make sure that a practical solution for industry is developed that is grounded in solid scientific research.

The work is organised along the following tasks:
Task 2.1: Increasing blade robustness: vortex generators (ECN)
A literature survey of the state-of-the-art in vortex generator modelling is first performed and candidates for incorporation in an Integral Boundary Layer method as in RFOIL are developed. Currently available numerical and experimental data are collected, used to develop the new VG model. A practical range of VG configurations is determined and the mathematical and numerical formulation of the selected approach is worked out and implemented in the current RFOIL code. Experimental data for airfoils with and without VG's from Task 2.4 is used to validate the implemented models.

Task 2.2: Increasing blade robustness: thick trailing edges (ECN)
A literature survey is first performed on thick trailing edge drag models. Experimental and numerical data is collected and used to create improved thick-TE drag model. This new model is implemented in the current RFOIL code. For extremely thick trailing edges possible numerical (convergence) issues in RFOIL are solved. Experimental data for airfoils with different trailing edge thicknesses from public domain and possibly from Task 2.4 is used to validate the implemented base drag model.

Task 2.3: High-fidelity CFD parameter sweeps (Siemens)
This activity starts with a definition of a matrix of numerical experiments that covers the required range of vortex generator and trailing edge thickness parameters; e.g. co-rotating and/or counter-rotating VG's, VG spanwise densities, VG height variations, VG streamwise alignments, Reynolds numbers, flow conditions, airfoil types, trailing edge heights. For this matrix of condition high-fidelity CFD simulations are performed and the full flow solution data near the airfoil is stored. From this data reduced quantities like lift, drag, and pitching moment are derived and the spanwise averaged development of integral boundary layer quantities like displacement thickness, momentum thickness, energy thickness, skin friction, etc. are determined. The results are used in Task 2.1 and Task 2.5 for model development and/or validation.

Task 2.4: Advanced blade section wind tunnel experiments (Siemens)
Airfoil geometries will be selected to be measured in the wind tunnel with and without vortex generators and possibly with different trailing edge thicknesses. A matrix of airfoil-VG configurations, flow conditions, and required measurement data are determined and a time schedule for the wind tunnel measurements is allocated. The wind tunnel tests are performed accordingly and the experimental data will be post-processed and analysed for further use. These results are used in Task 2.1 and Task 2.2 to validate the models implemented and possibly to enhance the model parameters afterwards.

Task 2.5: Vortex generator model development: CFD and wind tunnel experiments (TU-Delft)

The research aims at experimentally and numerically investigating the 3D flow of boundary layers with vortex generators, in order to develop both a model validation benchmark and a reduced order closure relation that can be used in integral boundary layer models and can be implemented in models such as RFOIL. The experimental results are developed at TUDelft boundary layer wind tunnel and the Low Turbulence wind tunnel, for both the cases of prescribed boundary layer flows with VGs and measurements on reference airfoils with VGs, including during stall and unsteady flow conditions (response to gust). The experimental methods involve high resolution Stereo PIV and Tomography, in order to capture the 3D vortical structures of the boundary layer and flow (both the average vertical structures and turbulence). The numerical flow field data from Task 2.3 is used and extended with CFD simulations for a range of parameters to create a vortex generator model for Integral Boundary Layer methods. From the numerical and experimental data, reduced quantities like lift, drag, and pitching moment are derived and the spanwise averaged development of boundary layer quantities like displacement thickness, momentum thickness, energy thickness, skin friction, Reynolds stresses and slip velocity, etc. are determined. The range of configurations covered in the numerical simulations is used to develop a vortex generator model and the experimental data are used to calibrate the model parameters. The resulting new vortex generator model is implemented in Task 2.1.

Task 2.6: Information and task coordination

A final Symposium on Vortex Generators is organized on 23-24 October 2017 to bring together experts from industry and academia from relevant sectors to discuss ideas and upcoming challenges, with a particular focus on new empirical findings, models and design methodologies.

1.3.3 WP3 Reduction of uncertainties by integral substructure design (ECN)

Background: To make offshore wind cost effective there is a need to reduce the cost of energy. The aim of this work package is to investigate where cost reductions in the support structure are possible while keeping a sound and safe design. Probabilistic design methods (structural reliability methods) are used to study whether there is any conservatism in the design of support structures.

At present, the design of support structures for offshore wind turbines is done in collaboration between the wind turbine manufacture and a specialized engineering company. The tower is designed by the wind turbine manufacture, while the foundation and sub-structure are designed by the engineering company. The support structure consists of a foundation, a sub-structure and a tower. The structural design is verified by applying partial safety factors as prescribed in the standards of Germanische Lloyd or DNV. Partial safety factors are applied to compensate for uncertainties in the design process, and improved knowledge may help to reduce these factors and hence contribute to reduction in COE without compromising the reliability of the design.

An alternative of applying (possibly conservative) partial safety factors probabilistic design methods will be applied. In the past probabilistic design methods were already used for wind turbines. For instance in the JOULE-III project PRODETO (PRObabilistic DEsign TOol) [1] the PhD-thesis of Veldkamp [2] and the work by Soerensen [3]. The focus in this work package is on the support structure while taking the complete offshore wind turbine system in to account.

Objective: enable cost reduction in the support structure by means of using a probabilistic design approach. The study will result in an improved understanding in the following:

- The safety level of an offshore wind turbine based on partial safety factors as prescribed in the standard;
- The safety level in case the life time of 20 years is increased;
- Identification of the importance of the different load parameters to the safety level.

The work is organised along the following tasks:

Task 3.1: Definition data base set up and selection of probabilistic methods and offshore wind turbines (ECN)
In order to investigate where cost reductions are possible in the support structure the loads and response (time) histories of an offshore wind turbine are needed. A state of the art reference offshore wind turbine is constructed in the project (D4REL turbine) and the loads and time histories of that turbine are calculated and stored in a data base. Before continuing with the next tasks the selected probabilistic method and the data base set up were presented to the advisory board.

Task 3.2: Creation of data base (ECN)
For the selected offshore wind turbine a data base is created by first modelling the wind turbine in Focus6 and then performing load calculations using the available aeroelastic tool Phatas. The quality of the data will be checked. Based on the analysis, it was decided to use a linearized model obtained with ECN's tool TURBU Offshore, instead of Phatas. The reason is that it offers a significant reduction of calculation speed while the loads were shown comparable to those from Phatas.

Task 3.3: Implementation of probabilistic methods (ECN)
Before a probabilistic analysis can be performed, the data needs to be processed by the selected probabilistic software tool.

Task 3.4: Probabilistic analysis (ECN)
Using the available data base and probabilistic tools, the safety level of the offshore wind turbines are analysed with respect to lifetime. Load parameters of the support structure design which are possibly important for cost reduction are identified.

Task 3.5: Re-assessment of safety factors (ECN)
Based on the probabilistic analysis, a re-assessment of the safety factors is performed and compared with the factors as prescribed in the standards.

Task 3.6: Assessment of industry questions (ECN)
During the project, requests from industry (Van Oord) related to the (probabilistic) design of support structure are expected. In this task, these questions are assessed.

1.3.4 WP4 System Identification for Robust Control (ECN, TU-Delft)

Background: Conventionally, wind turbine control algorithms are developed based on physical modelling of the control-relevant dynamics. Although this approach is intuitive and leads to simple (yet practical) control structures, the inherent uncertainty in the physical parameters involved in such "first-principles" models requires the use of conservative stability margins during the control design, associated with decreased overall controller performance. A noticeable improvement of the performance of the wind turbine controllers is expected to be achievable when more accurate (i.e. less uncertain) models are available. In WP4.1 system identification algorithms are developed that reduce the model uncertainties. The resulting less-uncertain models will be used in this WP4.2 to optimize the parameters of the wind turbine controller.

Objective: to increase the availability of wind turbines by means of using intelligent, self-adapting controllers in combination with improved information of the changing system parameter by system identification.

The work is organised along the following tasks:

Task 4.1 Nonlinear system identification with uncertainty quantification (TU-Delft)
While aeroelastic models are vital in the design stage of wind turbines to predict fatigue and extreme loads, power production and evaluate possible control systems, it is inevitable that many factors contribute to uncertainty or errors in the prediction of dynamic modes and time constants. Among those are: differences between expected and actual material properties; differences in manufacturing; differences in soil or foundation characteristics and modelling assumptions. These uncertainties result in suboptimal controllers and conservative safety factors. System identification may aid in better understanding the true underlying dynamics and, as a consequence, may be a key enabler for improvements to the design of controllers and the amount of conservatism of the different safety factors. There are two main open fundamental issues which further hamper the application of system identification for the wind community [4]. These two issues will be introduced below and are the main topics of this task.

- *Task 4.1.1. Uncertainty quantification*: System identification will reveal the underlying true dynamics of the wind turbine. However, since these techniques depend on a number of priors the estimated model will have a certain uncertainty. Descriptions of these uncertainties are hard to obtain for state-of-the-art wind turbine identification methods, which are based on the so-called subspace paradigm. While one could derive first order variance results for subspace methods, just as it is typically done for optimization based methods, it is unlikely that results will be reliable [5]. It seems that development of tailored Monte Carlo methods and bootstrapping techniques could be much more useful, such that based on a limited number of independent identification experiments a good characterisation of uncertainties can be found. The objective of this task is to develop an algorithm using randomized algorithms (such as bootstrapping) to add an uncertainty quantification to the identified model. This would, for instance, enable to estimate the structural damping of the support structure with uncertainty description for use in Task 4.2.
- *Task 4.1.2. Nonlinear system identification*: As wind turbines are nonlinear systems, current practice is to identify linear models in several operating points. However, since wind turbines operate in a continuously changing wind field it becomes hard, if not impossible, to obtain suitable data records for linear system identification, since large wind speed variations cause the linearity assumptions to be violated. The approach pursued here is to explicitly model the dominant nonlinear effects, enabling the use of arbitrary data obtained from the turbine under varying wind speed. The current state-of-the-art is to identify so-called Hammerstein (or interpolation) models which combine the static nonlinear behaviour with an LTI dynamic part [4]. It was also shown that this model structure doesn't capture all the dominant dynamics of a wind turbine. In this task, Linear Parameter Varying (LPV) will be used as it has a higher fidelity level and efficient controller synthesis techniques are available. However, for LPV system identification a computational traceable algorithm is still lacking. The objective of the work package is to develop an LPV identification scheme that beats the curse-of-dimensionality in state-of-the-art techniques by using tensor algebra. This will result in efficient data use and reduced uncertainty sets. Moreover, the framework developed in Task 4.1.1. will be extended to this model class.

Task 4.2 Self-adapting wind turbine control using identified models (ECN)
In contrast to conventional (off-line) controller design, system identification (Task 4.1) can be used continuously in an online setting, providing up-to-date information about important wind turbine parameters (e.g. frequencies of tower, drive train). Adapting the controller parameters to the changing turbine parameters will ensure constantly optimized and stable wind turbine controller. Such adaptive control schemes are developed in this task. They are particularly relevant offshore where the environmental conditions (e.g. water depth changes due to tides and/or scour, ice formation, etc.) can give rise to significant changes of the system parameters, which degrade the performance of the wind turbine controller.

Furthermore, this task also focuses on the development of condition based control algorithms, bridging the gap between existing condition monitoring (CM) schemes and the wind turbine control algorithms. In contrast to the "standard fault-tolerant control" approach, where action is taken after a failure has been detected, the condition based control approach pursued here aims at delaying an approaching failure to allow for maintenance to be planned and initiated before the failure actually occurs. A good example is the pitch mechanism, which due to its high failure rate is often one of the most important source of downtime. By detecting degraded performance (due to, e.g. increased friction, wear in the teeth, etc), the control law can be reconfigured so as to operate the turbine at reduced power, reducing the loading on the damaged part (e.g. the pitch mechanism). While keeping the wind turbine in operation, the loads reduction should delay the failure of the component, giving more time for planning and initiating (logistics, waiting time, travel time) the required maintenance activity.

Task 4.3 Evaluation of integral impact on CoE at system level (ECN, TU-Delft)
This is an integrating work package where the integral impact on cost of energy is determined of the technology that has been developed in the other work packages.

1.4 Project coordination

General meetings were held twice per year to inform the project consortium about the progress made in the project, and to facilitate cooperation between the partners. Due to the fact that participants from Siemens needed to travel to the Netherlands from Denmark, the meeting was hosted in Amsterdam. Generally speaking these meetings provided a platform to give feedback and enhance the research. A project website (www.d4rel.nl) was created and kept up-to-date, including information about the project scope, approach and achievements. In addition to that, a (protected) team site was established to facilitate the exchange of data and reports.

Besides organizing meetings and facilitating contact, the project coordinator has had its hand in steering the project results towards the defined deliverables, within the defined temporal and financial boundaries. Each year, a progress report was prepared and submitted to RvO. Having a foreign project partner abroad resulted in some "language issues" as some project related documentation was only available in Dutch and translation costs were incurred by the project coordinator to make the documents available to the foreign partners.

Technically seen, the project was executed according to plan. Some challenges during the execution were encountered in WP2, though. More specifically, besides the CFD and wind tunnel data provided by Siemens and TU-Delft to ECN, additional (and more detailed) data was needed by ECN to perform the modelling activities on vortex generators and thick trailing edges. Fortunately, ECN was capable to internally accommodate for the additional data needs. This did lead to some

delay in the modelling and its software implementation (RFoil) of the vortex generators and thick trailing edges. Fortunately, this delay was acceptable to the project partners (and Siemens in particular).

Organizationally, the main challenge was to ensure more collaboration between the different work packages due to the fact that there is barely any link between them in the agreed project plan. Due to this, possibilities for collaboration between the parties involved in different work packages were continuously and proactively sought already from the beginning of the project. To promote collaboration and search for new opportunities, this item was placed on the agenda of every project general meeting. Moreover, a document was created in the beginning of the project listing any foreseen, and possible, collaboration opportunities, and it was discussed and updated after every meeting. Although this activity did improve collaboration, the learning point here is that collaboration needs to be well established already in the proposal phase to ensure enough cross-fertilisation.

Another organizational issue was that the three PhD students of TU-Delft were found with some delay. The PhD student in WP1, Udai Shipurkar, actually started his activities as late as 11 months after the project start. This gave rise to a delay in the planned deliverables in WP1. This issue was reported in the progress reports already in 2014, and in 2016 a formal request for extension of the duration of WP1 with one year was submitted to RvO. This request was rejected. Fortunately, all PhD students (including Udai Shipurkar) managed to finalize all research activities and get their results before the end of the project. At the project end, their PhD theses are under preparation and are all expected to be finalized and defended in the period October 2017 - July 2018 (see Section 1.5.1).

Financially, the project is executed within budget.

1.5 Dissemination

Besides the numerous technical reports written, papers have been published in several journals and conferences. An overview of the dissemination events and publications is given below.

1.5.1 Project deliverable reports

1. U. Shipurkar and H. Polinder, Failure Avoidance in Wind Turbine Generator Systems, TU-Delft, August 2015, D4REL deliverable 1.2
2. U. Shipurkar, Fault Tolerance in Wind Turbine Generator Systems, TU-Delft, December 2016, D4REL project deliverable 1.3a
3. U. Shipurkar, Henk Polinder, Jan A. Ferreira, A Review of Methods to Increase the Availability of Wind Turbine Generator Systems, D4REL project deliverable 1.3b
4. U. Shipurkar, Henk Polinder, Analysis of Case Studies, TU-Delft, August 2017, D4REL deliverable 1.4
5. J. Steiner, H. Ozdemir, G. Bedon, A rotor blade section design capability that takes reliably into account the effects of vortex generators, ECN, August 2017, D4REL project deliverable D2.1.2
6. R. Vaithiyanathasamy, H. Ozdemir, G. Bedon, A rotor blade section design capability that reliably takes into account the effects of thick trailing edges, August 2017, D4REL project deliverable D2.2.2
7. P. Manjunath, ‘Simulation of low-profile vortex generator flow’, April 2016, D4REL project deliverables D2.3.2 & D2.5.4.

8. D. De Tavernier, 'Modelling of vortex generators within the integral boundary-layer theory', November 2016, MSc thesis, TU-Delft. D4REL project deliverables 2.5.5, 2.5.6 and 2.5.7.
9. Busra Akay, Wind Tunnel airfoil data, Siemens, January 2017. D4REL project deliverable 2.4.2
10. D. Baldacchino and C. Ferreira, 'Experimental investigation of low-profile vortex generators in a boundary layer wind tunnel', TU-Delft, April 2015, D4REL project deliverable 2.5.2.
11. D. Baldacchino and C. Ferreira, 'Experimental parametric study of vortex generators on the DU97W300 airfoil', TU-Delft, December 2016, D4REL project deliverable 2.5.3
12. D. Baldacchino. Aspects of vortex generator flow: fundamentals and practical insights (preliminary title), PhD Thesis (in preparation), Expected Early 2018. D4REL project deliverable 2.5.1 and 2.5.8
13. M. Asgarpour, J.M. Peeringa, Framework for Reliability Assessment of Offshore Wind Support Structures, ECN, February 2015, D4REL project deliverable D3.4.1.
14. B. Gunes and Jan-Willem van Wingerden, Report on Uncertainty Quantification, TU-Delft, June 2017, D4REL deliverable D4.1.1.2
15. B. Gunes, Jan-Willem van Wingerden and M. Verhaegen, Report on Non-linear System Identification, TU-Delft, June 2017, D4REL deliverable D4.1.2.1
16. U. Shipurkar, Improving the Availability of Wind Turbine Generator Systems (preliminary title), PhD Thesis (in preparation), Expected July 2018. D4REL project deliverable 1.5
17. Y. Gunes, A tensor approach to linear parameter varying system identification, PhD Thesis (in preparation), Expected January 2018. D4REL project deliverable 4.1.2.2
18. V. Pascu, Adaptation of controller parameters using identified models, ECN, June 2016, D4REL deliverable D4.2.1.
19. W. Engels, A. Marina, S. Kanev, D. van der Hoek, Condition based control, ECN, September 2017, D4REL deliverable D4.2.2.
20. S. Kanev and B. Bulder, Integral impact of the results from D4REL on the cost of energy at system level, ECN, September 2017, D4REL deliverable D4.3

1.5.2 Other publications and events

Journal papers

21. D. Baldacchino, C. Ferreira, D. De Tavernier, W. A. Timmer, G. J. W. van Bussel, Experimental parameter study for passive vortex generators on a 30% thick airfoil, Wind Energy, 2017
22. V. Pascu, S. Kanev and J.W. van Wingerden, Adaptive tower damping control for offshore wind turbines, Wind Energy, October 2016
23. B. Gunes, J.W. van Wingerden and M. Verhaegen. Predictor-based tensor regression (PBTR) for LTI, bilinear and LPV subspace identification. Accepted for Automatica, 2015.
24. B. Gunes, J.W. van Wingerden, and M. Verhaegen, Tensor nuclear norm LPV subspace identification. Conditionally accepted to Transactions on Automatic Control, 2016.
25. B. Gunes, J.W. van Wingerden, and M. Verhaegen, Tensor networks for MIMO LPV system identification. Submitted to International Journal of Control, 2017
26. G. Ramanujam, H. Ozdemir, H.W.M. Hoeijmakers, Improving Airfoil Drag Prediction, Journal of Aircraft, Vol. 53, No. 6 (2016), pp. 1844-1852.

Technical reports and theses

27. G. Ramanujam, Improving aerodynamic prediction methods for wind turbine airfoils, MSc thesis, University of Twente, 2016
28. V. Pascu, Reliable wind turbine control design, MSc thesis, TU-Delft, 2015. Published as ECN report number ECN-E–15-023.
29. V. Pascu, LMI-based robust LPV control for wind turbines, ECN, 2014. Report number ECN-E–14-036.

30. R. Vaithiyanathasamy, Double wake model for separated flows over airfoils, MSc thesis, University of Twente, 2017

Conference papers and presentations on events

31. U. Shipurkar and H. Polinder, Modularity in Wind Turbine Generator Systems – Opportunities and Challenges, 18th European Conference on Power Electronics and Applications (EPE'16 ECCE Europe), Karlsruhe, pp. 1-10, 2016.
32. Udai Shipurkar, Ke Ma, Henk Polinder, Frede Blaabjerg, Jan A. Ferreira, A Review of Failure Mechanisms in Wind Turbine Generator Systems, EPE ECCE 2015 Conference, 2015
33. G. Ramanujam, H. Ozdemir, H.W.M. Hoeijmakers, Improving Airfoil Drag Prediction, AIAA SciTech, Proceedings of the 34th Wind Energy Symposium, San Diago, USA, 2016
34. G. Ramanujam, H. Ozdemir, “Improving airfoil lift prediction”, Proceedings of the 35th AIAA wind Energy Symposium, Dallas, USA, January 2017
35. D. Baldacchino, M. Manolesos, C. Ferreira, Á. González Salcedo, M. Aparicio, T. Chaviaropoulos, K. Diakakis, L. Florentie, N.R. García, G. Papadakis, Experimental benchmark and code validation for airfoils equipped with passive vortex generators. In Journal of Physics: Conference Series, Vol. 753(2), p. 022002, September 2016.
36. D. Baldacchino, C. Ferreira, D. Ragni, G.J.W. van Bussel, Point vortex modelling of the wake dynamics behind asymmetric vortex generator arrays. In Journal of Physics: Conference Series, Vol. 753(2), p. 022025, September 2016.
37. D. Baldacchino, D. Simao Ragni, C. Ferreira, G.J.W. van Bussel, "Towards integral boundary layer modelling of vane-type vortex generators", Proceedings of the AIAA, June 2015.
38. D. Baldacchino, D. Simao Ragni, C. Ferreira, G.J.W. van Bussel, "Experimental investigation of asymmetric streamwise vortices in a turbulent boundary layer", Proceedings of 34th Wind Energy Symposium, Scitech 2016.
39. Johan Peeringa, Gabriele Bedon, Fully integrated load analysis included in the structural reliability assessment of a monopile supported offshore wind turbine, 14th Deep Sea Offshore Wind R&D Conference, EERA DeepWind’2017, 18-20 January 2017, Trondheim, Norway
40. B. Gunes, J.W. van Wingerden and M. Verhaegen. Tensor regression for subspace identification. Proceedings of American Control Conference (ACC), 2015.
41. B. Gunes, J.W. van Wingerden and M. Verhaegen. Tensor regression for subspace identification: free parameterizations. Proceedings of SYmposium on System IDentification (SYSID), 2015, p. 909-914
42. B. Gunes, J.W. van Wingerden and M. Verhaegen. Tensor regression for LPV subspace identification. Proceedings of SYmposium on System IDentification (SYSID), 2015, p. 421-426.
43. WindDagen 2016: TKI WoZ project D4REL
44. TKI WoZ Deelnemersbijeenkomst, 30 January 2015
45. Werkconferentie Topsector Energie, 5 November 2015, Utrecht.
46. R. Vaithiyanathasamy, H. Ozdemir, G. Bedon, A. van Garrel, A double wake model for interacting boundary layer methods, 36th AIAA Wind Energy Symposium, 8-12 January 2018, Florida, USA (accepted)

2. Technical achievements

In this chapter the technical achievements in the project are highlighted. For more detailed information, the reader is referred to the project deliverable reports, listed in Section 1.5.1.

2.1 WP1: Electrical Generator Systems for Reliability

Even though the reliability of wind turbines has improved over time, failure rates of more than one failure per turbine per year are observerd. Of these failures, the drivetrain is a major contributor. It is evident that addressing the failure rates of the drivetrain could have a major impact on the overall reliability of the wind turbine.

Objective:
The principal objective of the D4REL project is to improve the reliability and controllability of offshore wind turbines and thereby reduce the operational uncertainty of future offshore wind power plants. In particular, this work package (WP-1) aims at improving the availability of electrical generator systems.

Approach:
This objective is approached by organising the work package into the following tasks:

- Analysis of failure in generator systems.
- Study of fault avoidance.
- Analysis of fault tolerance.
- Selection of Case Studies.
- Analysis of improvement of availability for the selected case studies.

Based on this approach, three case studies have been selected to be analysed in detail. These are:

- Modularity in Generator Systems.
- Converter Topologies for Improved Lifetimes.
- Dynamic Thermal Management.

The highlights of the analysis of these case studies are given below.

2.1.1 Modularity in Generator Systems

Power electronic converters have been shown to be a major contributor to the failure rates of wind turbine drivetrains. This makes addressing their failures and improving their availability an important route towards reducing cost of energy. One method of doing this is through the

addition of modularity in the converter system. Modularisation is a design approach that decomposes a system into a number of 'modules' or components. The motivations behind the use of this concept have been diverse: from increasing manufacturability in machines, and standardisation of parts for the supply chain, to improving part load efficiency and system reliability. For wind turbines, this concept is attractive from the perspective of improving the availability of the turbine system predominantly in two ways. First, the introduction of fault tolerance, where the faulted module is bypassed and the remaining system continues operation with the same or a lower rating. Second, the increased maintainability of such a system, by making failed modules easier and cheaper to replace.

Objective:
The aim of this case study is to give a detailed overview of the effect of extreme modularity on the performance of a wind turbine generator system which could serve as a reference for future wind turbine designs that use large scale modularity in the generator system with the aim of maximising the availability of the turbine.

The contribution of this case study is that it extends previous work by investigating extreme modularity along with the effect of additional factors that come into play with such extreme modularity.

Approach:
This case study investigates the effect of modularity on the converter availability using Markov state space models to quantify these effects. The use of Markov modelling is one approach towards system level reliability modelling with the advantage that it is an effective tool for fault tolerant systems.

Results:
One method to reduce the operating cost of a wind turbine is to eliminate unscheduled visits and only allow periodic scheduled maintenance. This would require the fault modules to go 'off-line' while the healthy modules continue operation. All failed modules would be replaced in the periodic maintenance visit. Therefore, in this study only periodic maintenance is considered.

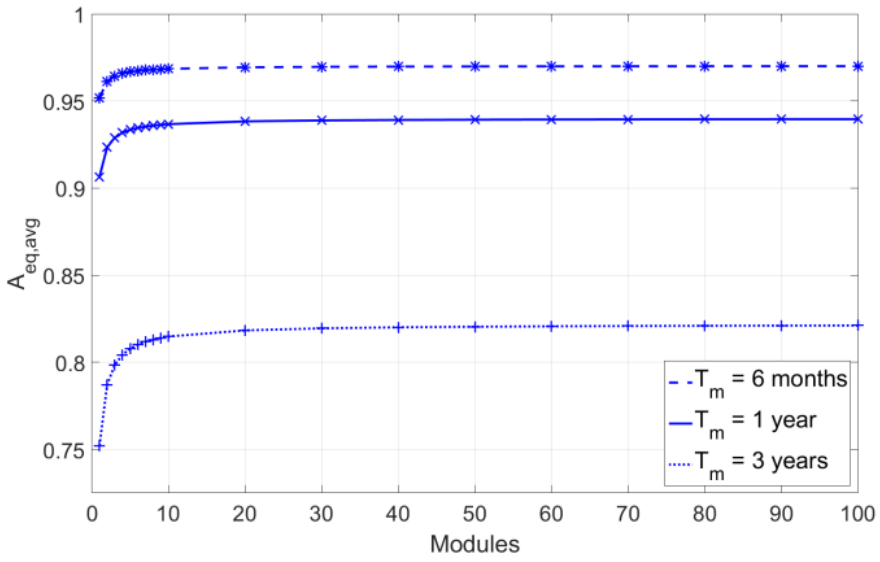

Figure 3 The effect of the number of modules on the effective availability averaged over one maintenance period for different maintenance periods and failure rate of 0.2 per turbine per year

An improvement in equivalent availability for modular systems requires some form of over-rating or redundancy. This results in a system that can handle a larger fraction of power than the fraction of modules that are healthy. As a significant portion of the operation of a wind turbines is with partial loading, the above requirement is met without the need of either over-rating or redundant modules.

The maintenance period (Tm) is an important consideration for the cost of energy of wind turbines. Enforcing periodic scheduled maintenance is a way of reducing maintenance costs. With this constraint, modular design can play a role in increasing the availability of the converter system. Figure 3 plots the availability over number of modules for three different periodic maintenance strategies.

The improvement in equivalent availability reduces with the addition of each additional module. This improvement varies inversely with the number of modules. With the number of modules exceeding 10-20, the improvements become such a small fraction of the availability that extreme modularity grants no significant benefit as seen from the figure above.

Another possibility is that the change in failure rates occurs due to a change in technology. Examples of this could be the cooling system where as the power rating of the converter module reduces, the cooling system can be changed from a liquid cooled system to an air cooled system and finally to a passively cooled system. Each of these technology change steps could reduce the failure rates as they involve removal of failure modes. According to a previous study [6], approximately 44% of the failures in the fully rated converters are due to the cooling system. With the introduction of extreme modularity, it is possible to implement thermal management for the converter using passive cooling. It can be hypothesized that this change would result in a reduction of the failure rate by approximately 44% as it eliminates a failure mode. A comparison of the annual energy yield when the number of modules are sufficient to allow passive cooling (N = Npassive) is presented in Figure 4.

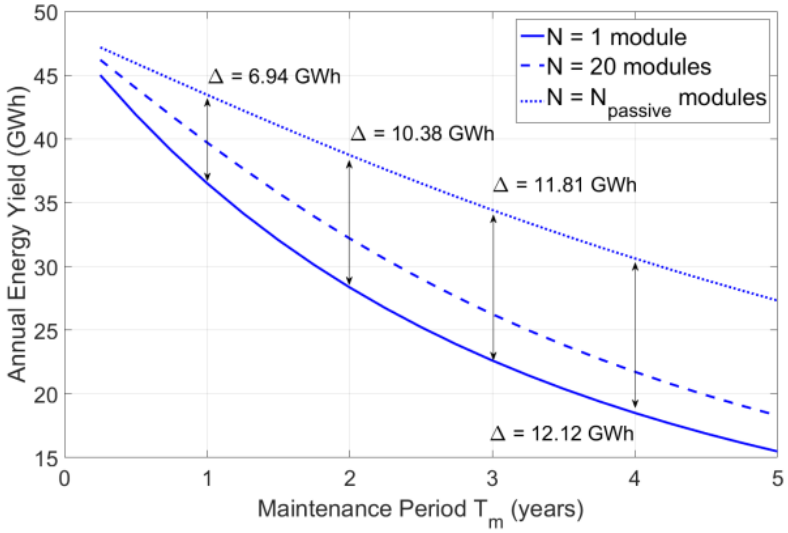

Figure 4 Annual energy yield with extreme modularity

Extreme modularity is now an option that merits consideration as it can lead to larger improvements in the equivalent availability.

Conclusions:

- For systems with continuous repair, modularity does not improve availability. In fact, modularity would increase the cost of repair as it would involve a higher number of maintenance visits.
- For systems with periodic repair, improvement in availability comes with some form of over-rating and modularity.
- As wind turbine systems often run at partial loading conditions, they are well suited to take advantage of this to improve availability without the need for either over-rating or redundancy.
- The improvement in availability reduces with each increment in the number of modules. The improvement after the number of modules exceeds 10-20 becomes insignificant.
- Extreme modularity is a viable option when it can lead to a reduction in failure rates and hence offer an improvement in the availability of the system

2.1.2 Converter Topologies for Improved Lifetimes

Conventional control schemes for wind turbines are based on the extraction of maximum energy from the wind. However, considering the cost of maintenance for far offshore wind turbines, it is important to look at reliability oriented design and control strategies that look to maximise the availability of the wind turbines rather than maximise the power production at each instant.

The section compares existing topologies like the NPC, A-NPC, H bridge, T-type from the point of view of reliability based on developed drivetrain, power semiconductor loss and thermal models. It further analyses the factors affecting the result of such a comparison.

Objective:
This case study investigates multilevel converter topologies with the view to compare different topologies with respect to their reliability. Although the range of multilevel converters can in theory be extended to any (2n+1)-level topology, this case study limits itself to a comparison of a number of topologies of the three level family. The three level topologies are chosen as they are the next step-up from the two level converters and address their issues while not complicating design and control to a large extent.

This case study extends the available comparisons to include the most prominent three-level topologies and modulation techniques, thus leading to a comprehensive comparison with the aim to draw overarching conclusions on the suitability of these topologies from the view of reliability. The contribution of this case study lies therefore in the variety of the 3-level converter topologies and modulation strategies that have been included in this comparative study. Further, these configurations are built into complete drivetrain models and judged on wind distribution over a complete annual cycle which gives rise to a realistic comparison.

Approach:
One method of comparing reliability is the use of handbooks to determine lifetimes of components and applying these to calculate system reliability. However, such methods have proved unreliable as they do not consider the mechanisms of failures and so cannot be used for all applications. An alternative is to use stress and strength modelling to map the loads that drive the failure mechanisms in the considered components and its resisting capability. This approach has been followed in this work. The assessment is developed based on the power losses of each converter, the distribution of these losses through their components and the impact that they have on the thermal behaviour of the power electronic components of each converter. The study

of the power loss and the thermal behaviour of the components offers useful conclusions about their lifetimes and the prospect of improving them.

With an aim to compare the lifetimes of power semiconductors in wind turbine converters, a detailed model of the wind turbine drivetrain is constructed. Figure 5 shows a schematic of the model.

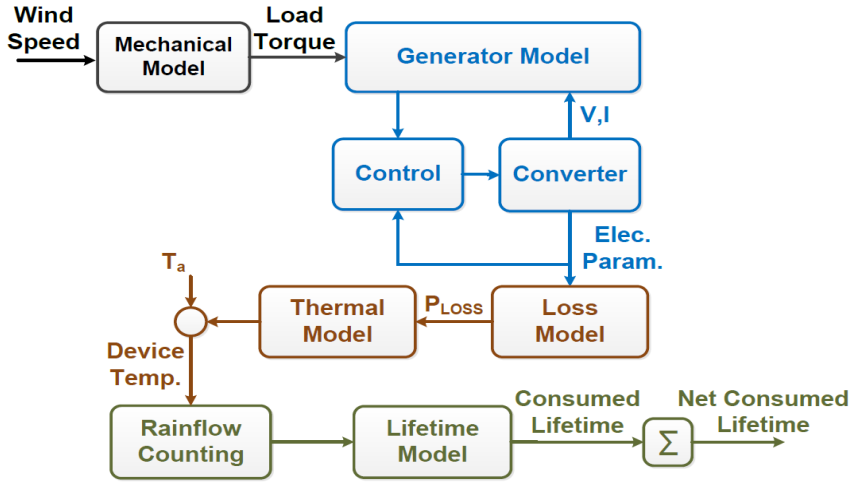

Figure 5 Schematic of System Model

Results:

As the converter reliability depends on the reliability of its weakest component, a topology that distributes the stresses more evenly amongst its components would result in a higher lifetime of the weakest component and hence the converter. Therefore, the loss distribution amongst the components is an important point of consideration. Figure 6 shows this loss distribution for the grid side converter operating at the rated wind speed point.

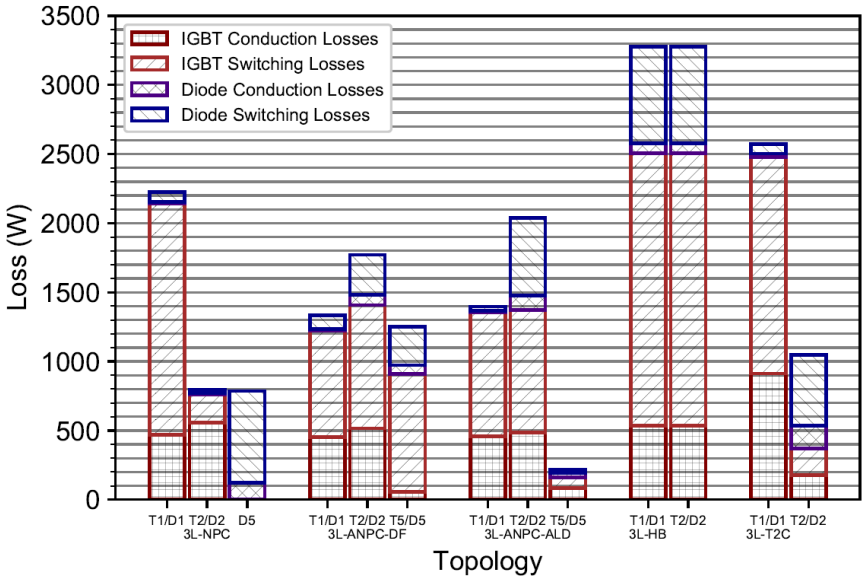

Figure 6 Loss distribution for the grid side converter with 12m/s wind speed

The thermal response of the power semiconductors to the losses that they are subjected to is closely linked to the reliability of each converter. In particular the junction temperature and the amplitude of the temperature cycling affect the lifetime of the power semiconductor. The

temperature cycling amplitudes of most stressed component in the grid side converter are shown in Figure 7.

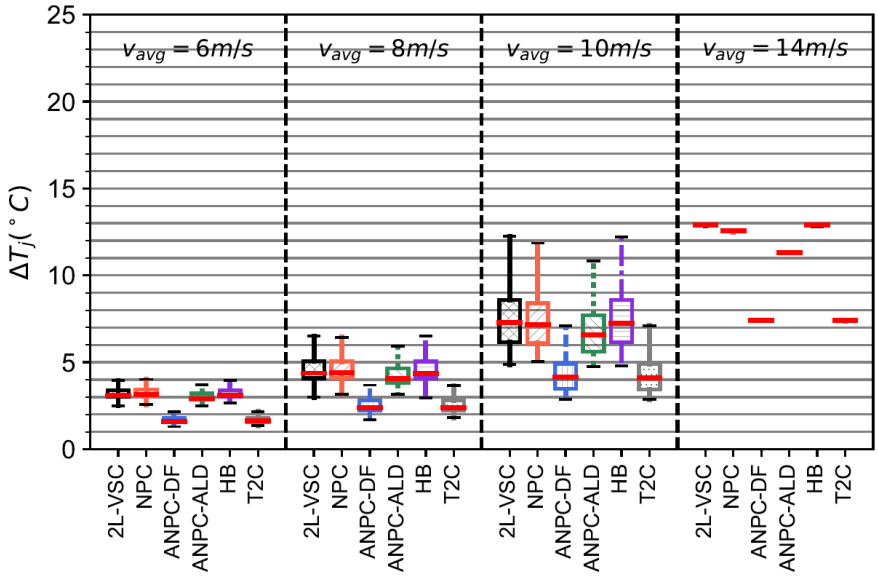

Figure 7 Distribution of temperature cycling amplitudes for the grid side converter

The 3L-NPC is a popular converter topology for high power wind turbine generator systems, therefore, it is important to also consider the effect of over-rating this converter to compare the improved lifetimes. This comparison is done for a 1.25 and a 1.5 overrated NPC topology (this results in a 5 and 6 parallel converter system) with the 3L-ANPC-DF and 3L-T2C converter topologies (with 4 parallel converters). The 1.5 times rated NPC topology results in a net IGBT rating equal to that of the 3L-ANPC and 3L-T2C topologies but a 50% overrating of the diodes. The resultant lifetimes for this comparison is given inTable 2.

Topology Lifetimes (in years)					
	Grid Side Converter		Generator Side Converter		Annual Losses (GWh)
3L-ANPC-DF	**57.49**	$(6.53X)$	**11.85**	$(7.37Y)$	0.96
3L-T2C	**110.08**	$(12.50X)$	**32.16**	$(20.02Y)$	1.13
1.25 x 2L-NPC	**28.33**	$(3.22X)$	**14.83**	$(9.23Y)$	1.00
1.50 x 2L-NPC	**63.69**	$(7.24X)$	**46.51**	$(28.95Y)$	1.05

Table 2 Comparison of lifetimes of the most stressed power semiconductors for topologies with over-rated 3L-NPC topology. X and Y represent the lifetimes for the base case 3L-NPC converter

Conclusions:

It has been found that in a comparison of different three-level topologies, the 3L-ANPC and the 3L-T2C show the highest lifetimes. When a component over-rating is considered, the 3L-NPC topology shows a large improvement and the lifetime performance is comparable to that of the overrated topologies. However, the loss performance of the 3L-ANPC remains marginally better than the other cases considered in this study.

In conclusion, the use of over-rating in the form of overrated topologies (like the ANPC and the T2C) or the use of overrated components is successful in improving the lifetime performance of

converters. However, the improvement offered by overrated topologies over the use of overrated components is not significant and it is unlikely to replace the current practice of using overrated components.

2.1.3 Dynamic Thermal Management

Junction Temperature and Junction Temperature Cycling are two major driving factors of failure mechanisms in power semiconductors. Previous studies have shown that active control concepts such as power sharing, reactive current circulation, DC-link regulation, modulation strategy, and active gate control can successfully increase the lifetimes of the power semiconductors in converters by reducing junction temperature cycling. Another possibility is the use of controlled dynamic cooling to reduce the amplitude of temperature cycles.

The dynamic thermal management system uses the modulation of the flow rate to reduce temperature cycling amplitudes. When junction temperature reduces, the system reduces flow rate, thus making the cooling system less efficient, thereby reducing the amplitude of the cycle.

Objective:
This case study analyses controlled dynamic cooling of power semiconductors for wind turbine drivetrains. It addresses the control structure of such a system, the issues in measuring or estimating the junction temperature for control.

The contribution of this case study is that it explores a method of increasing lifetime of power semiconductors, that has only been proposed before and has not been analysed in detail.

Approach:
The analysis is carried out on the basis of simulations on analytical models of a power semiconductor and heat sink system. The simulations consider the thermal response of the system to a cyclical power loss in the semiconductor. In a real system, this power loss would be the result of power cycling. Control of the system is based on a control structure as shown in Figure 8.

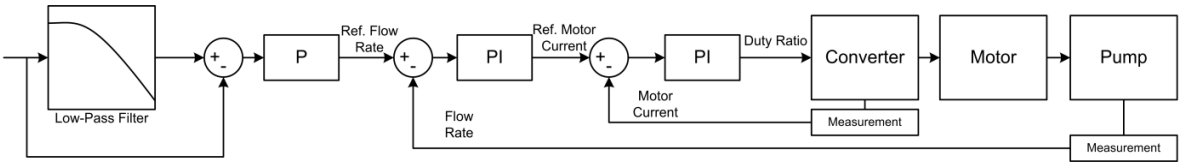

Figure 8 Control Structure

Results:
The control structure can be based on the junction temperature, the case temperature, or the heat sink temperature. The use of the case and heat sink temperature has the advantage that these parameters can be measured directly, while estimating/measuring the junction temperatures is difficult. However, performance is best when junction temperature is used as the control parameter.

Results for a cyclical loss amplitude in steps of 50W up to a net amplitude of 250W per IGBT, with a base loss of 250W is shown in this document. The junction temperature of a system with a control based on the structure defined in Figure 8 and Figure 9 is shown in Fig. 7. This is based on a simulation study with a power cycling.

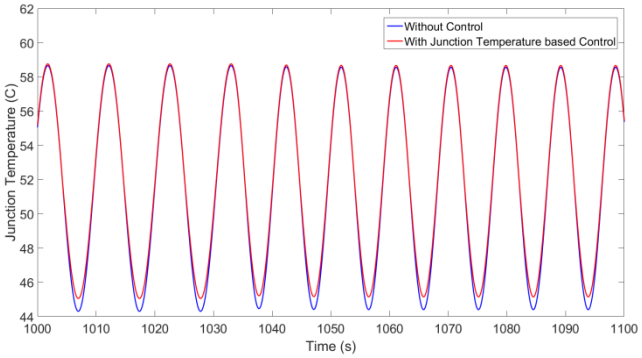

Figure 9 Junction temperature with and without dynamic thermal management

Figure 10 shows the reduction in temperature cycling amplitude for the case when the control is based on the junction temperature of the power semiconductor.

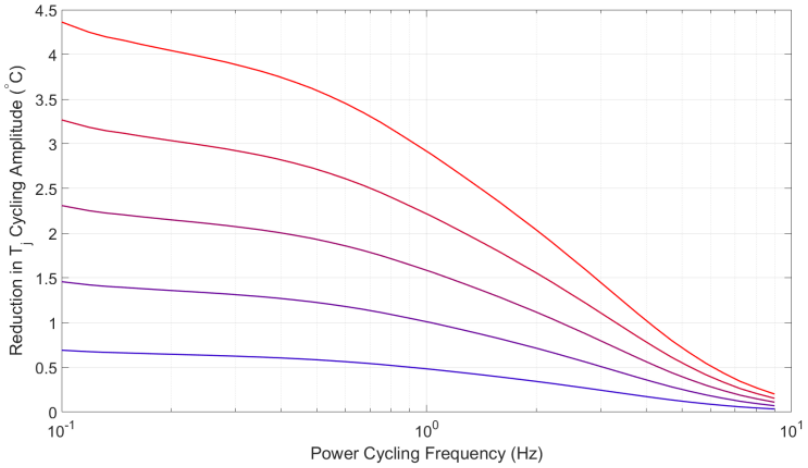

Figure 10 Reduction in amplitude of junction temperature for a cyclical loss amplitude

To further quantify the effect of this reduction on the lifetime of the semiconductor, a lifetime model based on the work by Bayerer et al. is used [7]. The inverse of the cycles to failure gives the damage caused by each cycle. Figure 11 gives the reduction in damage for both the case when the control is based on the junction temperature of the power semiconductor.

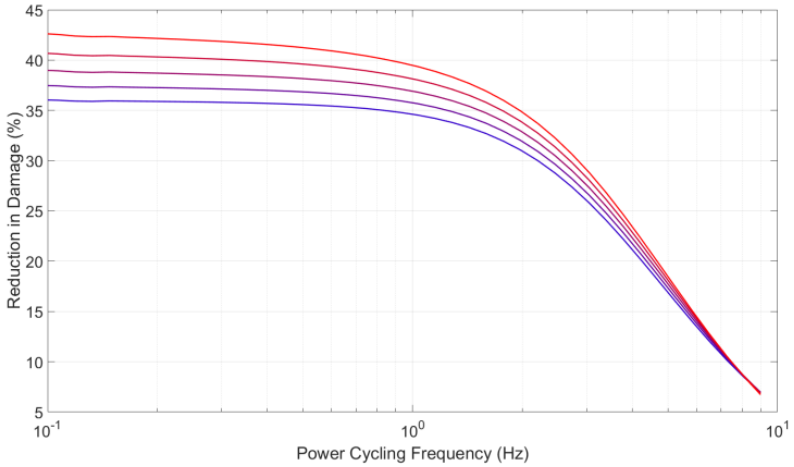

Figure 11 Reduction in damage per cycle of loss variation for a cyclical loss amplitude

Conclusions:

- As most wind turbine converters today use liquid cooling for the power semiconductors, the use of controlled dynamic cooling could play a significant role in reducing stresses and increasing lifetimes.
- The dynamic thermal management based on control of junction temperature performs better than when case temperature is used. However, estimating/measuring the junction temperatures is difficult, while case temperature can be measured directly.
- It is indicated that using such a system could reduce the damage of the power semiconductor between 0 – 40% depending on the conditions considered.

2.2 WP2: Next generation of robust offshore blades

Motivation and Goal

The overall objective of WP2 is to generate the knowledge and design capability that enables the development of the next generation of larger and lighter offshore wind turbine blades that do not rely on failure prone features and thereby lower the cost of energy. More specifically, this work package enable the accurate and reliable simulation of the effects of vortex generators and thick trailing edges (Figure 12) on wind turbine performance by extending the existing airfoil design tool RFOIL with models for the effect of vortex generators and thick trailing edges on airfoil aerodynamic performance that are validated against experimental data. From numerical and wind tunnel experiments flow field data will be obtained and analysed to create a vortex generator model that will be implemented in RFOIL. Partners in this work package ECN, Siemens, and TU Delft make sure that a practical solution for industry is developed that is grounded in solid scientific research.

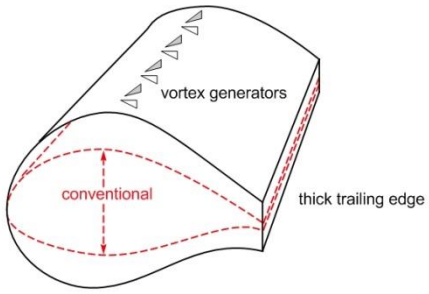

Figure 12 A sketch of vortex generators placed on an airfoil with a thick trailing edge

2.2.1 Task 2.1 Vortex generators and Task 2.3 CFD parameter sweeps

This study mainly focuses on the effect of the vortex generators on the boundary layer properties. To this purpose, a matrix of numerical experiments that cover the required range of vortex generator is defined; e.g. co-rotating and/or counter-rotating VGs, VG spanwise densities, VG height variations, VG streamwise alignments, Reynolds numbers, flow conditions, airfoil types, trailing edge heights. For this matrix of condition high-fidelity CFD simulations is performed and the full flow solution data near the flat plate is stored. From this data the spanwise averaged development of integral boundary layer quantities like displacement thickness, momentum thickness, energy thickness, skin friction, etc. is determined.

Approach

The aim of this study is to capture the effect of a standard delta vortex generator on the boundary layer properties of a typical blade section relevant to wind energy applications using CFD. Due to time constraints, only one vortex generator/airfoil section combination will be examined. In doing so the plan is to touch upon the following objectives:

- Provide detailed data of the boundary layer properties for the uncontrolled and controlled case for different operational conditions of the wind turbine. The data is to be used for the integration of vortex generators in the in-house implementation of Rfoil. The inclusion of vortex generators in Rfoil will make it possible to optimize the airfoil shapes with the vortex generators with much less computational power required as compared to CFD. Moreover, since Rfoil is fine tuned for this application it is generally expected to perform better than CFD especially for thick airfoils.
- Validation of the CFD solver of choice at ECN, namely SU2, for lift and drag prediction, as well as vortex generator simulation through comparison with available measurement data and CFD data available from literature.

To accomplish this, first a brief literature review has been performed alongside with a 2D mesh convergence study for the chosen airfoil. Next, the vortex generator mesh is constructed using the flat plate reference case for the mesh convergence study. Subsequently, full 3D simulations are performed for a selection of angles of attack. Lastly, a thorough evaluation of the obtained data is performed with special regards towards calculation of the integral boundary layer properties.

Validation cases

The choice of the specific test case is mostly determined by the openly available measurement data. Sources for tripped data for the clean and controlled case are limited. Thus, measurement data from an old measurement campaign in Riso is used [8]. While the Reynolds number of the measurements is contained to 1.6 million and as such lower than desired, it is considered a good starting point for validation of the results.

In Figure 13 lift and drag polars for the controlled and uncontrolled case are shown. For comparison also the smooth leading edge measurements are shown not just the tripped cases.

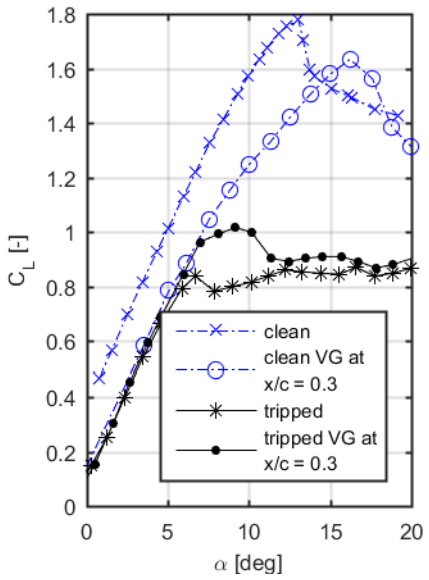

Figure 13 Lift and drag polar for the FFA-W3-301 airfoil at Re = 1.6m

Results

Vortex generator mesh

The 2D topology of the vortex generator mesh is shown in Figure 14. Note that due to the no slip condition along the device surface, the mesh has to be refined all around the vortex generator. This makes the meshing procedure quite complicated and very sensitive to changes in resolution. The 2D geometry is then projected onto the boundaries of the spanwise section to create the 3D block structure. Finally, the desired wall spacing is imposed towards the VG surface, overall 60 nodes were used in spanwise direction.

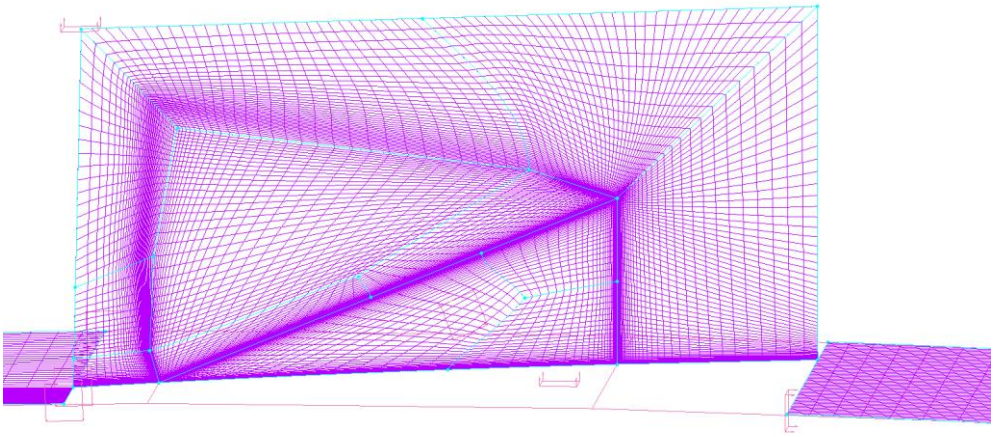

Figure 14 Vortex generator 2D basis mesh

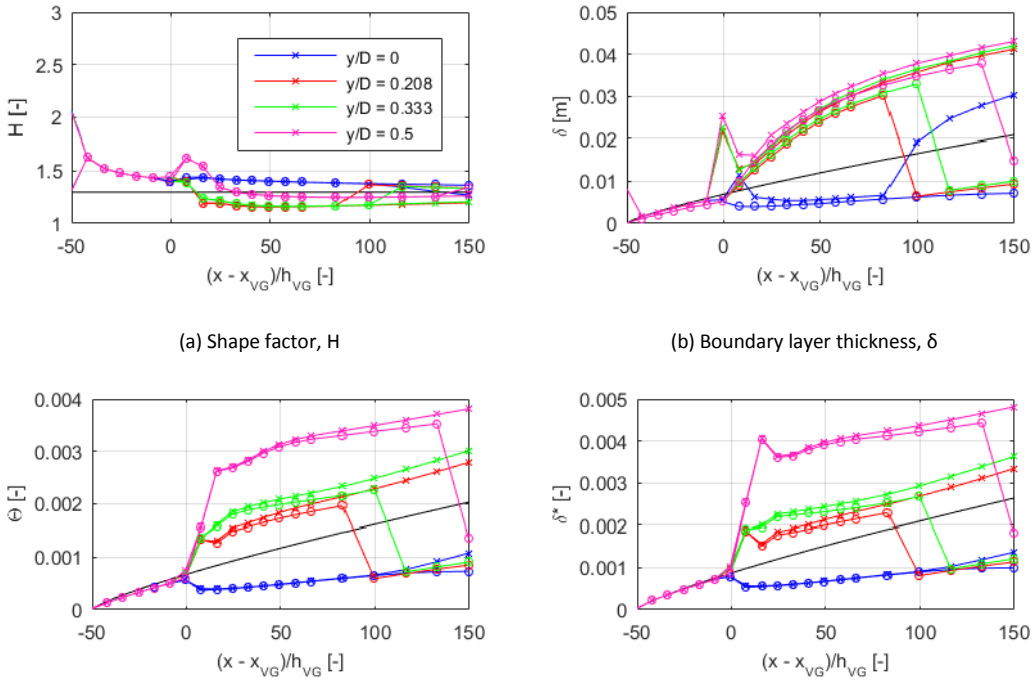

(a) Shape factor, H

(b) Boundary layer thickness, δ

(c) Momentum thickness, θ

(d) Displacement thickness, δ*

Figure 15 Integral boundary layer properties as calculated from SU2 simulation for the controlled flat plate alongside analytical solution for the flat plate (black), where (x) refers to the vorticity method and (o) to the vorticity/shear combined method for the determination of the boundary layer edge

Evaluation of boundary layer properties

Flat plate:
The results from the three different methods for the clean flat plate benchmark case are compared in Figure 15.

Airfoil:
The vorticity threshold and the combined shear and vorticity threshold methods are applied to the clean 3D airfoil simulations. The results are shown in Figure 16 for an inflow angle of 12 degrees. While there is some difference between the predictions of the boundary layer height, little to no difference is observed in the calculation of the integral boundary layer properties.

The comparison between SU2, Xfoil and Rfoil for one constellation is also shown in Figure 16. First off, different closure models are used in Rfoil and Xfoil. In Rfoil, if the flow starts separating, a limit is imposed on the momentum and displacement thickness, thus here the increase in the shape factor indicating separation is not captured. Nevertheless, as was visible from the polar comparison earlier, Rfoil is more accurate in predicting lift and drag than Xfoil. Other than that, the boundary layer properties are qualitatively well captured. However, as already seen from the polar plot lift is overpredicted in SU2 which results in an underprediction of the separation region as compared to measurements as well as Rfoil.

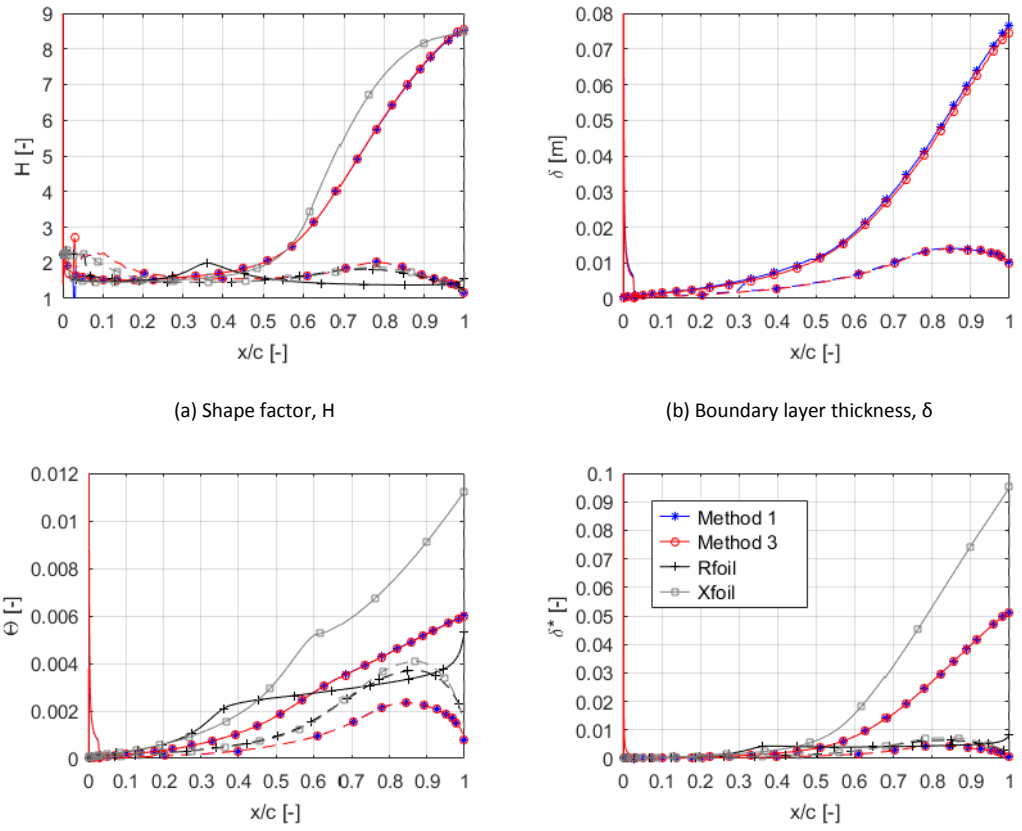

(a) Shape factor, H

(b) Boundary layer thickness, δ

(c) Momentum thickness, θ

(d) Displacement thickness, δ*

Figure 16 IBL properties as calculated from SU2 alongside Rfoil and Xfoil for the uncontrolled, tripped airfoil at AoA = 12 deg and Re = 1.6m where the pressure side is marked by the slashed line

In Figure 17 the one on one comparison between the uncontrolled and the controlled case for an inflow angle of 12 degrees is shown. Both methods for the determination of the boundary layer edge are tested. However with some adjustments to include irregular velocity profiles the first

method works much better. The third method fails once the irregularities in the velocity profiles are not that pronounced anymore and thus then substantially underpredicts the boundary layer thickness. This can already be seen also for the flat plate case in Figure 17. Thus in the following only the minimum vorticity threshold method will be used. For the sake of simplicity also only the suction side will be presented, since the pressure side is only indirectly influenced by the vortex generator via induction from the wake.

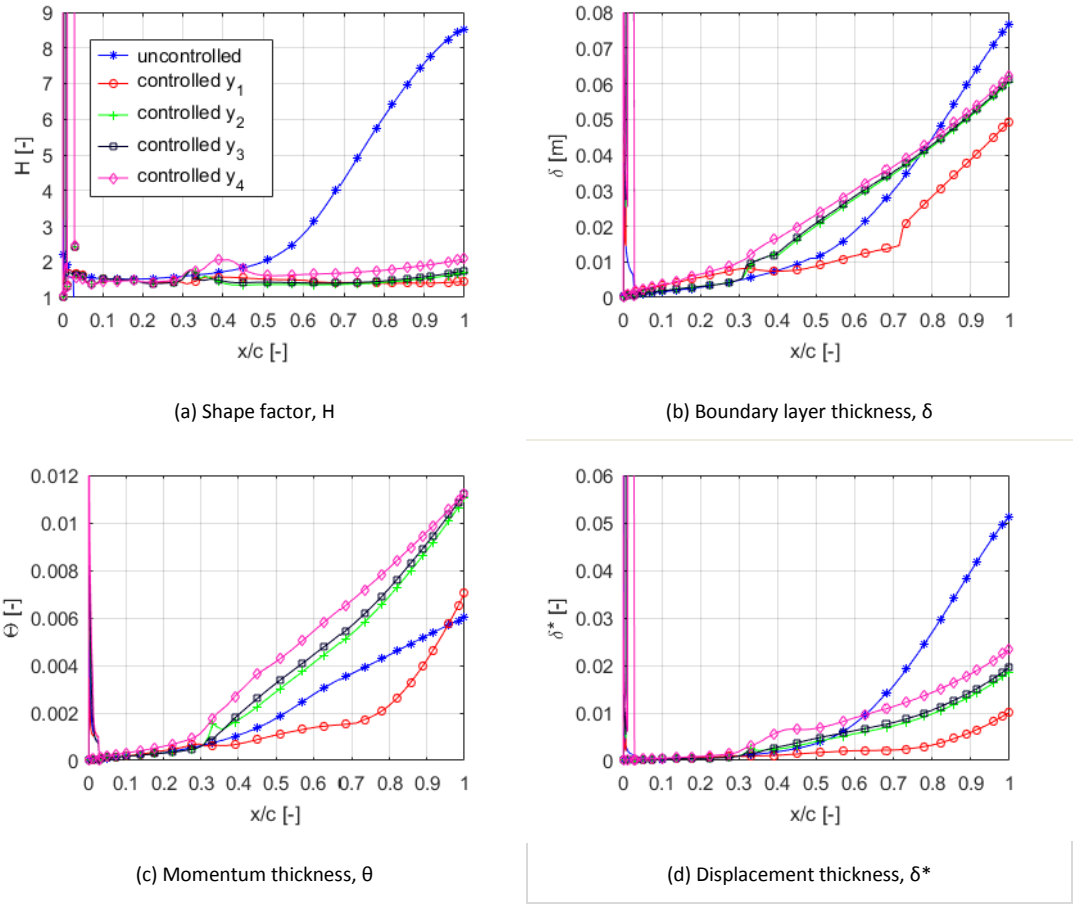

(a) Shape factor, H

(b) Boundary layer thickness, δ

(c) Momentum thickness, θ

(d) Displacement thickness, δ*

Figure 17 IBL properties as calculated from SU2 for the uncontrolled and controlled tripped airfoil with the vortex generator position as x / c = 0.3 at AoA = 12 deg and Re = 1.6m, only the suction side is presented

Velocity profiles

Vortex generators produce characteristically S-shaped velocity profiles in streamwise and cross-streamwise direction. This is also qualitatively well captured by SU2 as can be seen in Figure 18.

The results are compared with velocity profiles obtained for an experimental setup on a non-adverse pressure gradient flat plate case by Baldacchino et al [9]. Even though for this specific reference case no adverse pressure gradient is present, the main characteristics of the velocity profiles agree well with each other. Namely, the general S-shape of the velocity profiles and the slow decay in intensity of the curvature compare well. Also, the cross-streamwise perturbation of the flow decays much faster than the streamwise one due to the increased opposition from the main flow.

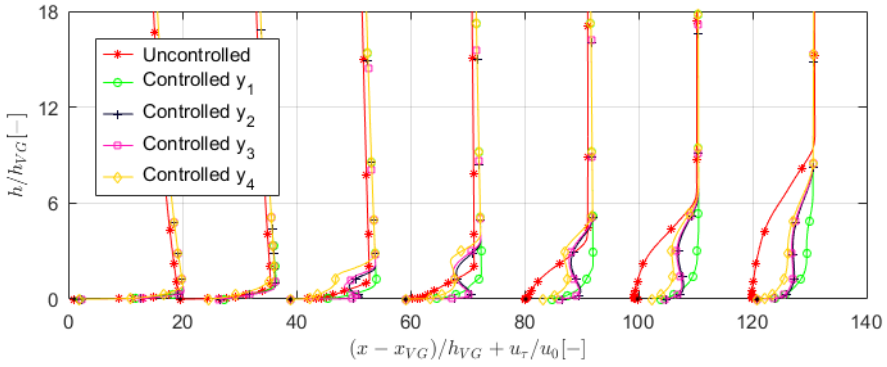

(a) Shape factor, H

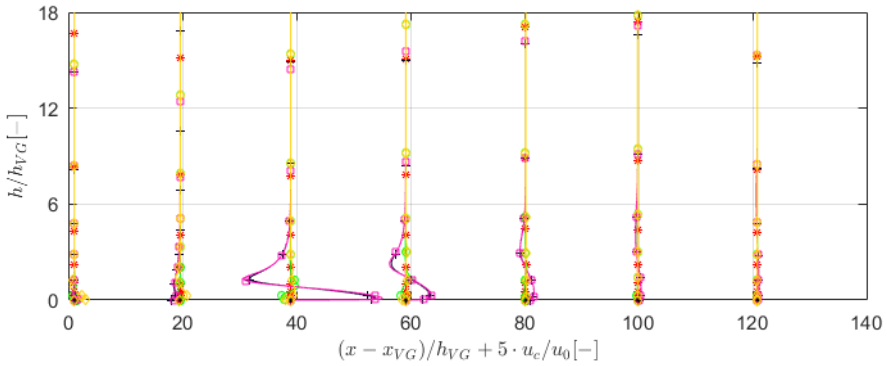

(b) Boundary layer thickness, δ

Figure 18 Velocity profiles downstream of the vortex generator for the uncontrolled and controlled airfoil section at AoA of 12 deg and Re = 1.6m

Vortex formation

The development of the main vortex induced by the vortex generator in terms of path, radius and intensity can be seen in Figure 19 where the streamwise vorticity is used as an indicator. While the plot is only qualitative, one can see how the vortex lifts away from the surface with increasing downstream coordinate. Moreover, the vortex radius also increases while the circulation slowly decreases through viscous dissipation in the vortex core. However, even at the trailing edge while not very pronounced anymore the vortex is still visible.

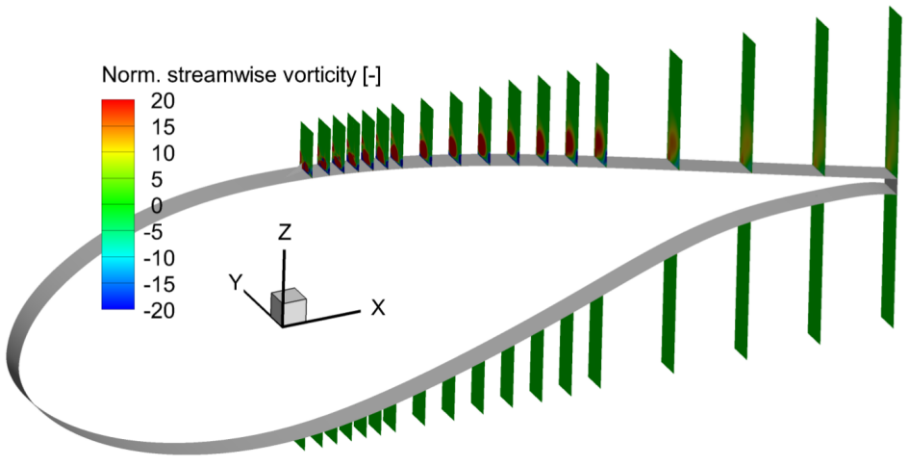

Figure 19 Illustration of the vorticity development of the SU2 simulation results at AoA = 12 deg and Re = 1.6m

In Figure 20, a more detailed view on the different vortices around the device is shown. An experimental study of the different vortex systems around a vane vortex generator for different heights and relative inflow angles was carried out by Velte et al [10]. The findings distinguish between three different systems of vortices according to their origin, namely

- A strong primary vortex P induced through the shape of the vortex generator.

- A horseshoe vortex (HS, HP) around the vortex generator, which is only formed if the adverse pressure gradient produced through the vortex generator is strong enough [11]. The vortex arm on the suction side HS of the device will either be swept underneath the primary vortex or smeared along the wall through the induced velocity of the primary vortex.
- A secondary opposite oriented vortex structure S induced by the primary vortex due to wall vortex interaction will also form given a high enough circulation of the primary vortex. If the vortex is especially strong i.e. at high relative inflow angles and large height of the device a second vortex D can even form through the same mechanism [11]. The experimental study shows that this vortex will be swept to the other side of the primary vortex [10].

Moreover, the results also suggest three different prevalent combinations of those vortices further downstream of the device as a function of the device height and inflow angle.

Now looking at the results from SU2, the identification of the different vortices is not straight forward. First of all, here a delta vortex generator is used whereas for the experiments a vane vortex generator was used. Intuitively speaking, the vane vortex generator is expected to produce stronger horseshoe vortices than the delta shaped one due to the stronger produced adverse pressure gradient. Secondly, the experiment only investigated device heights up to the boundary layer height. However, for the shown constellation the vortex generator height is slightly higher as compared to the uncontrolled case. Thus as such the primary vortex is expected to be stronger than for the reference case, of course this should also result in a stronger secondary vortex system due to viscous effects. Thirdly, for the experiments only a single vortex generator on a flat plate without adverse pressure gradient was tested. Thus the induction of the primary vortex from the second device of a device pair will also not be represented by the measurements [11].

The interpretation of the different vortices according to the nomenclature by Velte et. al. [10] also denoted in Figure 20. One can see that the horse shoe vortices are not very strong and especially HP dissipates rather quickly. However, especially the placement of the secondary vortex system is quite different from what was observed in the reference [10]. Thus, this is either due to the lack of the second vortex generator in the measurements or possibly also the result of the symmetric boundary conditions in the CFD simulations. Also there are two very small vortices on top of the primary vortex, whose origin is unclear. One explanation is that these are two more induced vortices of the secondary vortex system.

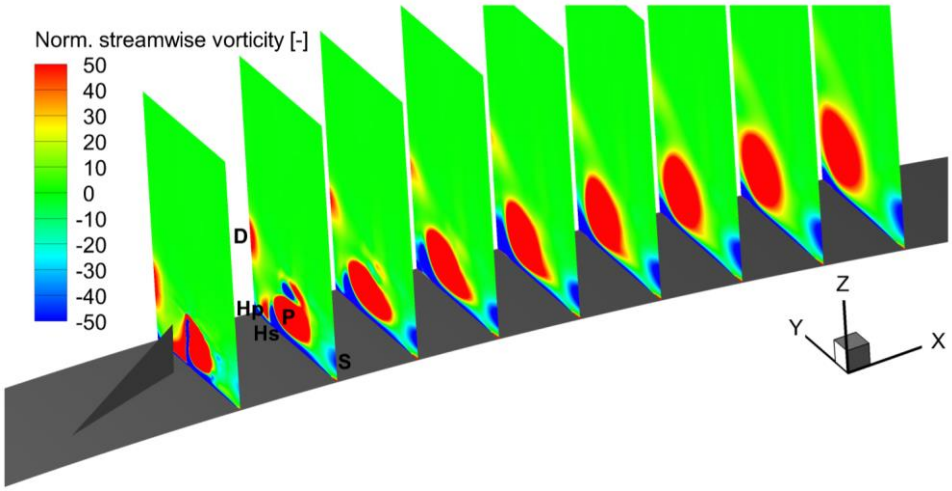

Figure 20 Illustration of the different vortex formations around the control device as obtained from SU2 at AoA = 12 deg and Re = 1.6m

2.2.2 Task 2.2 Increasing blade robustness: thick trailing edges

Objective

RFOIL is an engineering model for aerodynamic design of airfoils developed by ECN, NLR and TU Delft that is based on XFOIL. RFOIL has radial flow corrections, an addition of Coriolis and centrifugal force (rotational effects) to the boundary layer, which solves steady state flows implementing a single wake from the trailing edge of the airfoil. This gives acceptable predictions for attached flows and flows with moderate separation. However, for flows with high separation the prediction of lift from RFOIL needs to be improved. One of the ways this can be done is by incorporating the continuous vorticity emitted at the separation point in the form of additional wake (i.e. double wake implementation). The main objective is to develop an inviscid double wake model which could be later coupled with the viscous effects.

In engineering tools, panel method is used to model the inviscid flow around the airfoil using a doublet/vortex singularity elements. In the classical inviscid panel method, a single wake from trailing edge is released. The integral boundary layer equations are then solved using source terms on the airfoil surface and the wake, to get the mass deficit and account for the streamlines displacement away from the surface. Then the viscous effects are incorporated with the obtained inviscid solution using one of the available viscous-inviscid coupling procedures. In the proposed double wake implementation method for RFOIL, the second wake is released from the separation point in addition to the primary wake at the trailing edge to model the inviscid flow region. Then the source terms need to be coupled to get the mass deficit and eventually the final solution. The separation point required for modelling the second wake has to be given externally. The idea of double wake implementation can be extended to both conventional sharp trailing edge airfoils and blunt trailing edge airfoils. As the double wake model is developed to be implemented in the aerodynamic design tool RFOIL, all the illustrations that are referred below will be based on RFOIL.

Research approach and methodology

- Learning panel method, RFOIL source code and previous works on double wake models.
- Creating FORTRAN algorithm to model inviscid flow using 2D panel method.
- Validating the model with industry standard tools.
- Developing inviscid double wake model to represent the separated flow over airfoils.
- Testing and validating with experimental and numerical results.

Inviscid double wake model

The single wake inviscid model describes the inviscid flow region. This could be combined with the integral boundary layer equations to model the viscous effects for the attached flow. Once the separation sets in, double wake inviscid model could be used to model the effects of the separated flow region. This is due to the nature of the separated flow. Vorticity representation gives useful information especially when the flow separates. In the viscous region i.e. inside the boundary layer, there exists velocity gradient and so vorticity is formed. The formed vorticity cannot be destroyed and so it is convected and diffused in the flow. In the outer flow regime, i.e. the inviscid region, there is no velocity gradient and so no vorticity is formed. When the flow separates, all the vorticity that is formed in the viscous region is convected downstream from the separation point and from the trailing edge. This convected vorticity can be modelled with the help of wake sheets emanating from the separation point and from the trailing edge with vorticity strength. Based on Kelvin's circulation theorem, in a potential flow, vortex sheet established at any instant remains the same at all instances of the time. This consequence of Kelvin's theorem is utilized to model both the wakes as constant vortex sheet and to find the solution iteratively. In this region between the two wakes, the vorticity is negligible leading to negligible losses and so total pressure remains

constant. This indicates that there is no shear layer in the region between the two wakes. Therefore, from the separation point until the trailing edge, the flow can be assumed to be purely inviscid. Hence, double wake inviscid model holds good to represent the separated flow region. However, the non-separated flow region over airfoil in separated flow requires the combination of panel method and the integral boundary layer equations to model the viscous effects. The double wake inviscid model can be done for both conventional sharp trailing edge and blunt trailing edge airfoils.

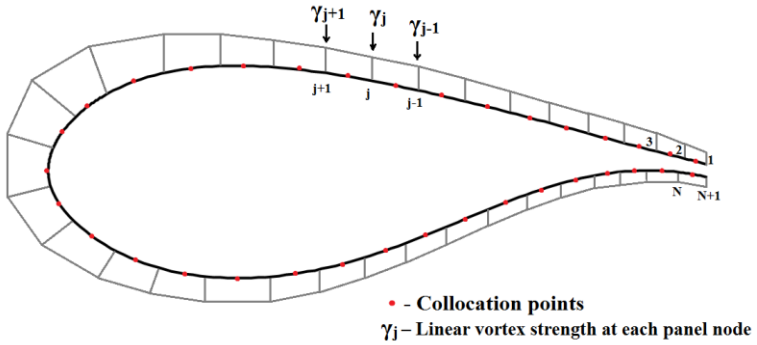

Figure 21 A sketch of linear vortex strength distribution on airfoil surface with blunt trailing edge used for initial wake shapes calculation

To model the secondary wake, the separation point needs to be known. It is given as an external input for the double wake inviscid model. The point of separation can be taken from experiment or found from viscous flow either from XFOIL or RFOIL. (When the double wake inviscid model is implemented in RFOIL, the separation point will be found at the first iteration of RFOIL simulation). To set up the vorticity strength on the wake, the initial wake shapes are required. The initial wake shapes are determined as streamlines from the induced velocities as a result of linear vortex singularity elements distribution over airfoil surface panels. The linear vortex distribution over airfoil surface is used and is shown in Figure 21 for thick trailing edge airfoils. The same formulation is used for conventional sharp trailing edge airfoils.

The solution is obtained by applying vorticity of constant strength on the wake panels. The vorticity strengths on the airfoil and wake panels can be iteratively calculated with the Neuman boundary condition on the collocation points including the vorticity strength of the wake sheet. The wake shape is recalculated for subsequent iterations based on freestream velocity and induced velocities from airfoil and wake vorticities. The near wake panel of the initially formed wake from separation point is at very high angle with respect to the airfoil. This means the flow does not leave the airfoil surface smoothly. The solution is iterated with the trailing edge wake and separation wake vorticity influence over airfoil vorticity distribution until the near wake panels from the separation point leaves the airfoil surface smoothly. Further, the accuracy of the solution obtained depends on the chosen number of wake panels and in turn the wake length. The number of wake panels for the following analysis is fixed to be 500, higher than the number for which no influence of the wake panels on the final solution is registered. The obtained initial wake and the final wake after convergence, from separation point and trailing edge is shown in Figure 22for NACA63415 airfoil at an angle of attack of 160 and Reynolds number of 160, 000.

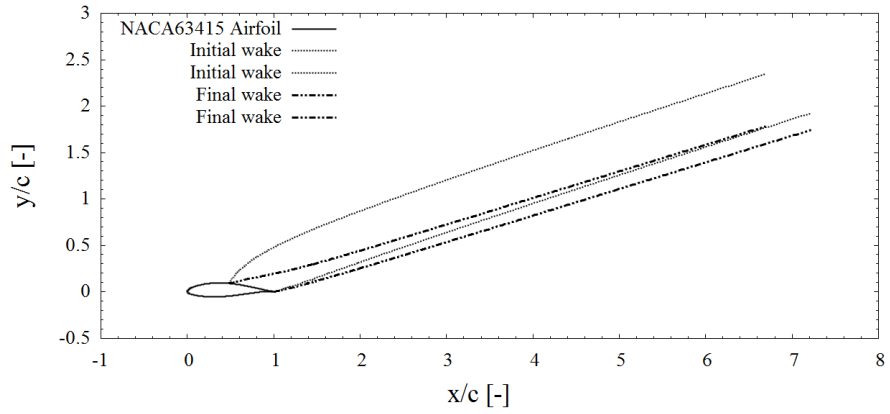

Figure 22 Initial and final wake shapes of NACA63415 airfoil

Pressure coefficient

The flow inside the airfoil is stagnant and so the tangential velocity is given by the airfoil surface vorticity, in the absence of source terms as described by Drela. The inviscid pressure coefficient distribution can be calculated from the known vorticity distribution from the airfoil surface. When the flow separates, there is a jump in total pressure across the separation wake streamline from the non-separated flow region which is added to the pressure coefficient.

Validation cases with sharp trailing edge airfoils

Figure 23 shows the comparison of pressure coefficients with the current inviscid double wake model, XFOIL, CFD and experimental data for S826 airfoil at Reynolds number of 100,000 and at angle of attack of 14.50. The separation point for the inviscid double wake method is located at x/c=0.43 and is obtained from experimental data. It can be seen that the inviscid double wake method can replicate result closer to that of experiment and better than the numerical viscous solution of XFOIL, in the separated flow region. However, it has to be considered that feeding the separation point from experiment gives added advantage to the inviscid double wake model. The peak suction pressure from the inviscid double wake method is largely over-predicted. It has to be noted that the inviscid double wake model has the disadvantage of not having viscous effects. Further, the release of wake from separation point gives a small oscillation at the separation point.

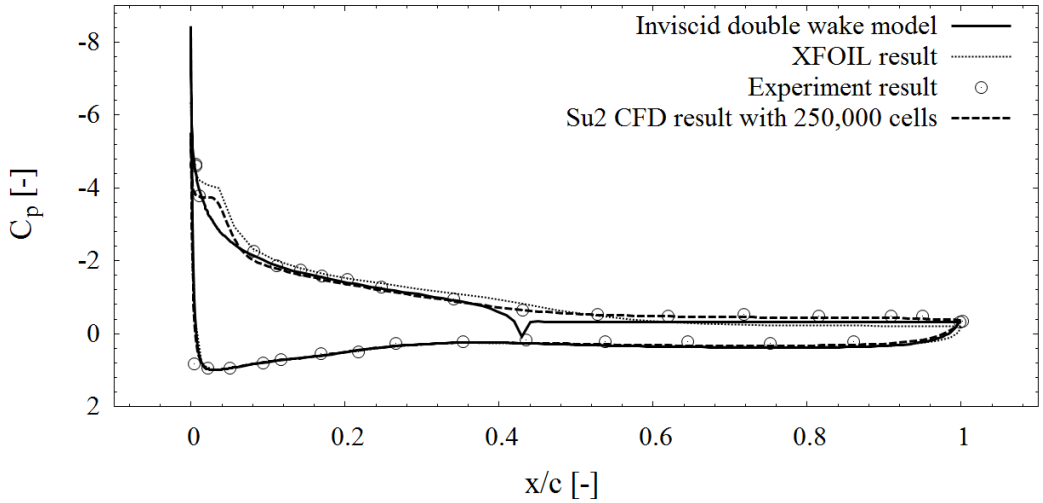

Figure 23 Pressure coefficients of inviscid double wake model for S826 airfoil with experiment, XFOIL and numerical result at Re=100, 000 and at angle of attack of 14.5^0

Validation case with blunt trailing edge airfoil

Result for blunt trailing edge airfoil is shown in the Figure 24 using FFA-W3-301 30% thick airfoil. The plot shows the pressure distribution obtained from inviscid double wake model along with the

experiment and XFOIL results at Re=1.6*106 and angle of attack of 16.70. The experimental data is obtained for the smooth flow over the FFA-W3-301 airfoil. The separation point for the inviscid double wake method is located at x/c=0.41 and is obtained from experimental data. It can be seen that the pressure distribution in the separation region can be captured to a very good accuracy when compared to experiment. The inviscid double wake model gives more accurate result than XFOIL viscous simulation. However, it has to be considered that feeding the separation point from experiment gives added advantage to the inviscid double wake model. Further, the release of wake from separation point gives a small oscillation at the separation point.

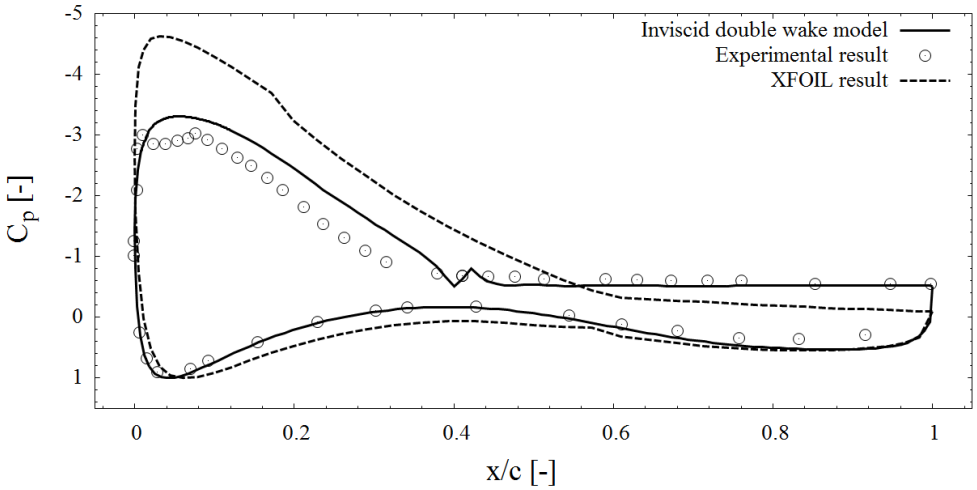

Figure 24 Pressure coefficients for FFA-W3-301 airfoil of inviscid double wake model with experiment and XFOIL result at Re=1.6*10^6 and angle of attack of 16.7^0

Conclusions and further work

From the results, it is evident that the inviscid double wake model can give better pressure distribution than XFOIL in the separated flow region with separation point fed from the experimental data. This indicates that the inviscid double wake model is capable of predicting good results if the separation point is known accurately. Also, this method can reproduce results closer to that of experimental and numerical CFD results in the separated flow region. From the initial wake shape to convergence, it takes 4 to 6 iterations to get the final results.

There are few shortcoming of this double wake inviscid approach. Firstly, the small hump occurs at the separation point due to the wake release. Secondly, in the non-separated flow region, the calculated pressure distribution lacks accuracy in comparison to the experiment or numerical data as there are no viscous effects. These deficits can be overcome by coupling the double wake inviscid model with the viscous effects which is explained later in the section. The other limitation is that the separation location has to be provided externally for the double wake inviscid model. The separation point can be obtained from the first iteration of single wake inviscid-viscous calculation (RFOIL) where the skin friction becomes negative indicating flow separation for steady state solution. However, for high angle of attacks, this is not feasible due to convergence failure with single wake inviscid-viscous calculations.

The results show that the pressure distribution is predicted very accurately in the separated flow region. Hence, the implementation procedure as described below is followed in RFOIL for all the airfoils. As the region enclosed between the double wake has negligible vorticity, no velocity correction is required from the viscous flow for the separated region. Figure 25 and Figure 26

show the viscous-inviscid solution scheme for RFOIL and coupling of viscous effects with the double wake inviscid model, respectively.

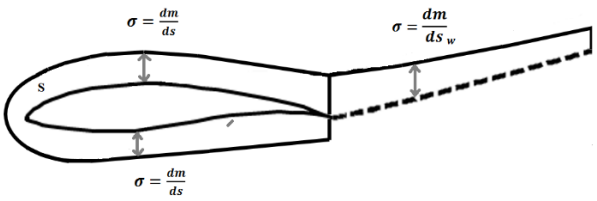

Figure 25 RFOIL viscous-inviscid scheme

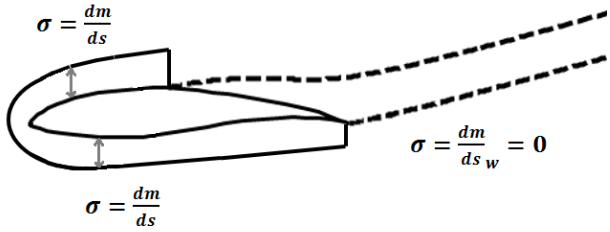

Figure 26 Viscous coupling with double wake inviscid model

2.2.3 Task 2.4 Advanced blade section wind tunnel experiments

Summary

In the frame of D4REL project, Siemens Wind Power A/S provided wind tunnel experimental data to ECN in order to perform the validation of RFOIL model for vortex generators and moreover for thick airfoils and thick trailing edge airfoils. The provided experimental data is summarized in Table 3.

Airfoil name	Transition	VG	Re	Airfoil thickness/chord	Trailing edge thickness/chord
SWPNA2_2412	Free/Forced	w and w/o	3e6	24%	0.2%
FFA-W3-301	Free/Forced	w and w/o	3e6	30%	2%
SWPNA06_3505	Free/Forced	w and w/o	2.5e6	35%	5%

Table 3 Experimental data provided by Siemens to ECN in the framework of D4REL project

All the wind tunnel data was obtained in TU Delft low speed low turbulence wind tunnel by measuring the surface pressure and wake rake pressure between approximately -20° to +20° angles of attack at every angle (see Figure 27).

Figure 27 TU Delft Low speed low turbulence wind tunnel [12]

The low speed low turbulence wind tunnel is an atmospheric tunnel of the closed-throat single-return type. The six-bladed fan is driven by a 525 kW DC motor, giving a maximum test section velocity of about 120 m/s. Due to the large contraction ratio of 17.8, the free-stream turbulence level in the test section varies from only 0.015% at 20 m/s to 0.07% at 75 m/s [12].

The tests were performed in an octagonal test section of 1.80 m wide, 1.25 m high and 2.60 m long. The airfoil models, having 1.25m span and maximum 0.9m chord length can be fit on the mechanically actuated turntable which enables to change the angle of attack during the test.

The provided data includes Cl, Cd and Cm distributions at every measured angle of attack together with the surface pressure and wake rake pressure distributions. The airfoil profiles were also provided along with the pressure distributions. Moreover, CFD data was provided for SWPNA06_3505 airfoil. Pressure and velocity fields around the airfoil were provided at 4 different angles of attack with both free and forced transition conditions.

The provided data was aimed to be used in the analysis of VG impact. Moreover, t/c=30% and 35% thick airfoils provide insight about the thick airfoil analysis. SWPNA06_3505 could also be used for the thick trailing edge analysis.

Data analysis

In Figures 28, L/D versus angle of attack distributions are presented for the airfoils which the experimental data were provided.

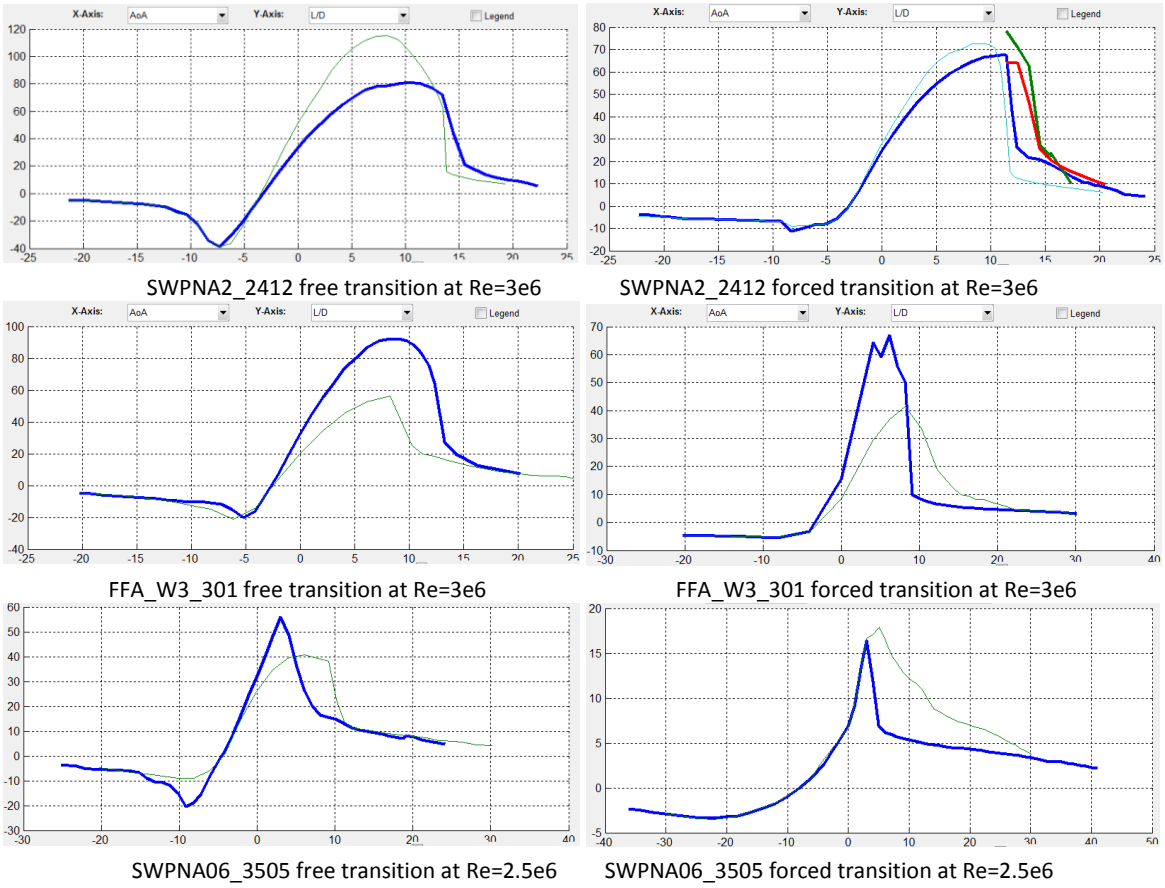

SWPNA2_2412 free transition at Re=3e6 SWPNA2_2412 forced transition at Re=3e6

FFA_W3_301 free transition at Re=3e6 FFA_W3_301 forced transition at Re=3e6

SWPNA06_3505 free transition at Re=2.5e6 SWPNA06_3505 forced transition at Re=2.5e6

Figure 28 Cl/Cd distributions for the airfoils used in the experimental study

2.2.4 Task 2.5: Vortex generator modelling: CFD and wind tunnel experiments

Database and benchmark of existing data

Experimental wind tunnel measurements conducted at the Low-Speed Tunnel of TU Delft by Timmer and van Rooij [13] were included for an Re range of $1 - 2.0 \times 10^6$. The experimental data available is for the following airfoil sections:

- DU 91-W2-250 (25%c thickness)
- DU 93-W-210 (21%c thickness)
- DU 97-W-300 (30%c thickness)

For each airfoil section the following configurations were measured:

- Clean airfoil data (No VGs)
- Controlled airfoil: triangular, vane-type vortex generators on the upper airfoil surfaces. General VG properties are as indicated below in Figure 29.

For the DU 91 and DU 97, additional data combining Gurney Flaps and zigzag tape were also provided. This contribution comprised part of a larger database used for model development and calibration.

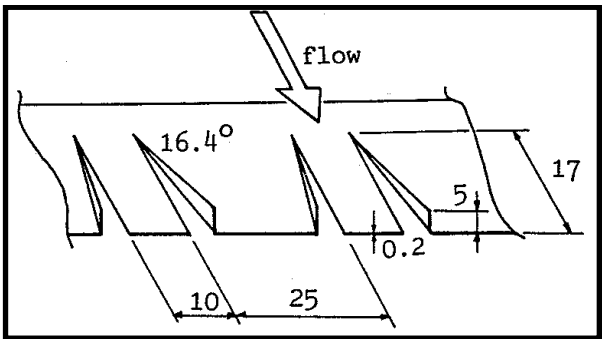

Figure 29 VG configuration. Dimensions in [mm]

Development of a VG model for IBL codes

The industry workhorses that are integral-boundary layer type codes currently lack a model for the effect of vortex generator to assist with integral blade design. To this end, an engineering model was developed using the extensive experimental database generated in Tasks T2.1 and 2.4, as well as additional experimental and computational reference input data from literature.

The method models the effect of a streamwise vortex by adding a source term to the integral shear-lag equation. This effectively mimics the increased dissipation of the vortex. The value of this source term is quantified with a brute-force optimisation approach for a range of VG and flow parameters (Figure 30 and Figure 31). The source term integral, in the spirit of IBL codes, synthesizes both the vortex strength and decay, allowing the definition of a single-valued empirical relation. This determines the required VG-added impulse for a given combination of user-defined, independent variables. The form of the source term, I_{ST} is

$$C_0 . \left(\frac{h_{VG}}{l_{VG}}\right)^{C_1} . (l^*_{VG} sin\, \beta_{VG})^{C_2} . (U_{VG})^{C_3}$$

The results are verified and validated for cases outside the model calibration database. Predictions are fair, as sampled in Figure 32. The device drag is not modelled in the current implementation and the calibration cases did not evenly cover the range of independent variables. Therefore results are more uncertain for the following design variations: array packing density, internal vane spacing and vane shape.

Experimental Parameter Study

An experimental parametric study was conducted for a wide range of VG parameters on a typical wind turbine airfoil – the DU97W300, at $Re = 2 \times 10^6$. The measurements were conducted in the Low Turbulence Tunnel at Delft University of Technology. The problem was approached pragmatically: a reference design was chosen, to which all the parametric variations were compared. This ensured a realizable test program without sacrificing the quality of the campaign. Over 40 test cases were considered, covering:

- VG shape parameters (length, height, shape)
- Mounting strip influence
- Chordwise placement
- Array configuration
- Boundary layer state

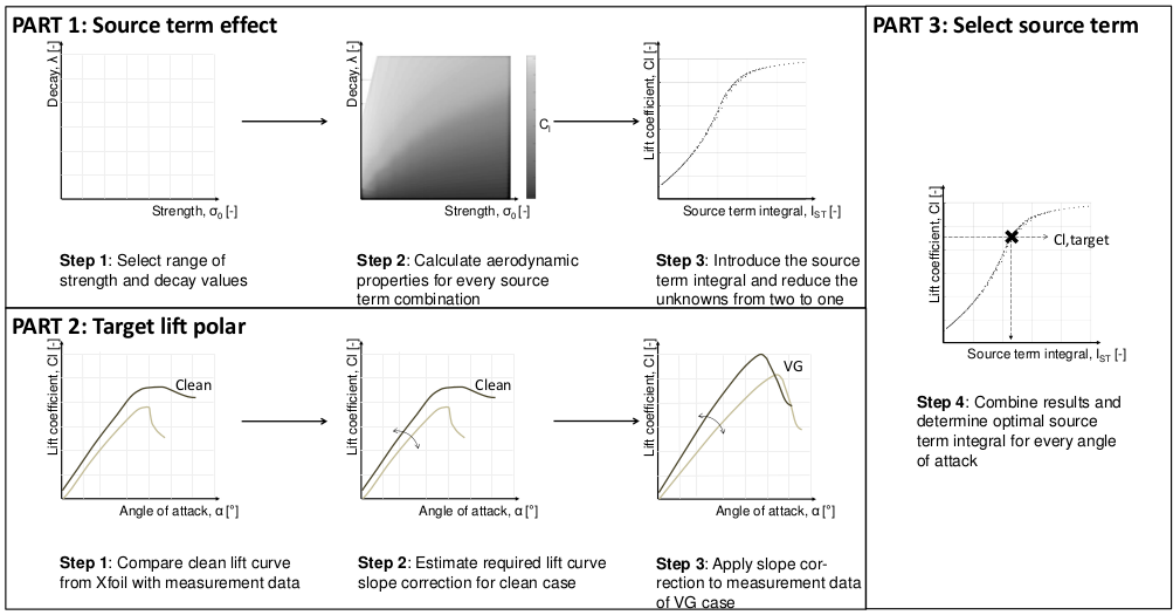

Figure 30 Source term optimisation approach

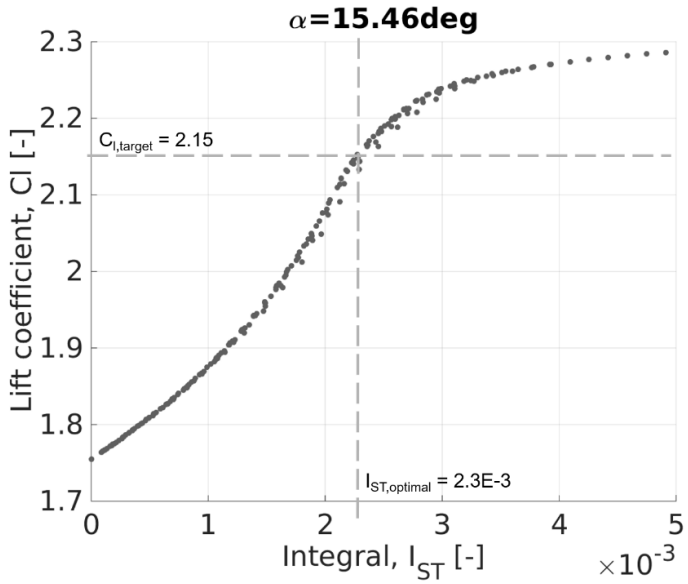

Figure 31 Optimal source term integral identification

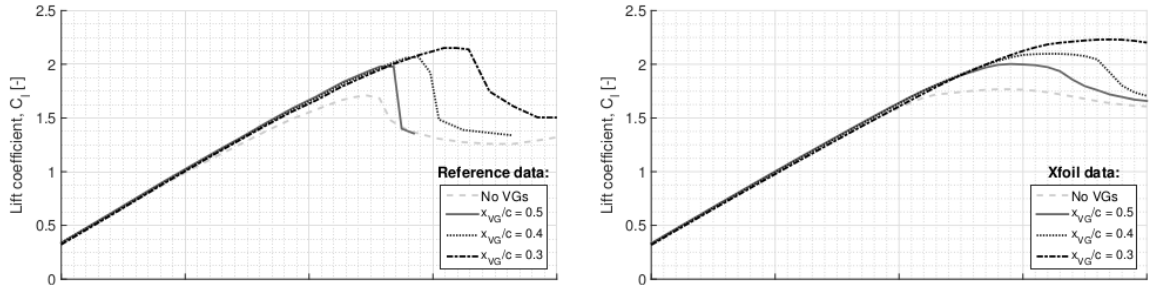

Figure 32 Influence of the VG array chordwise location on the performance of the DU97W300 airfoil. Experiment (left) and XFOIL (right)

The initial design calculations were verified using airfoil boundary layer measurements, whereas oil-flow visualisations confirmed the efficacy of the VGs (Figure 33). The results may be summarised as follows:

- The effect of the mounting strip is to increase the base drag and cause early turbulent separation, thereby reducing maximum lift (Figure 34).
- The array position, configuration and vane heights were of primary influence.
- Vane shape, angle, length and array packing density were of secondary influence.
- The VGs were able to offset the performance detriment due to simulated roughness.
- The load fluctuations in stall are significantly stronger in the presence of VGs (Figure 35).

The study further demonstrated the design of effective passive flow control devices using existing tools (XFOIL/RFOIL) and provided accurate measurement data. This was made available for model generation, calibration and validation.

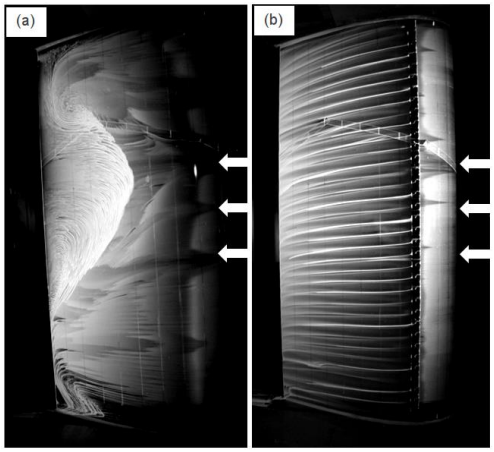

Figure 33 Oil flow visualization of the DU97W300 at an angle of attack of $\alpha = 14°$; (a) without and with (b) vortex generators mounted at 20% chord. Flow from right to left.

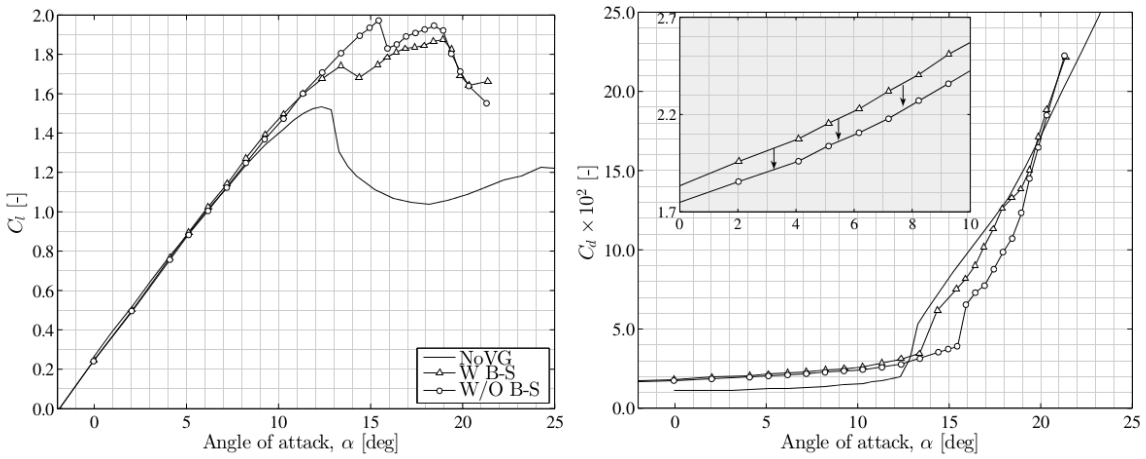

Figure 34 Influence of the base-strip: With Base-Strip (W B-S) & Without Base-Strip (W/O B-S)

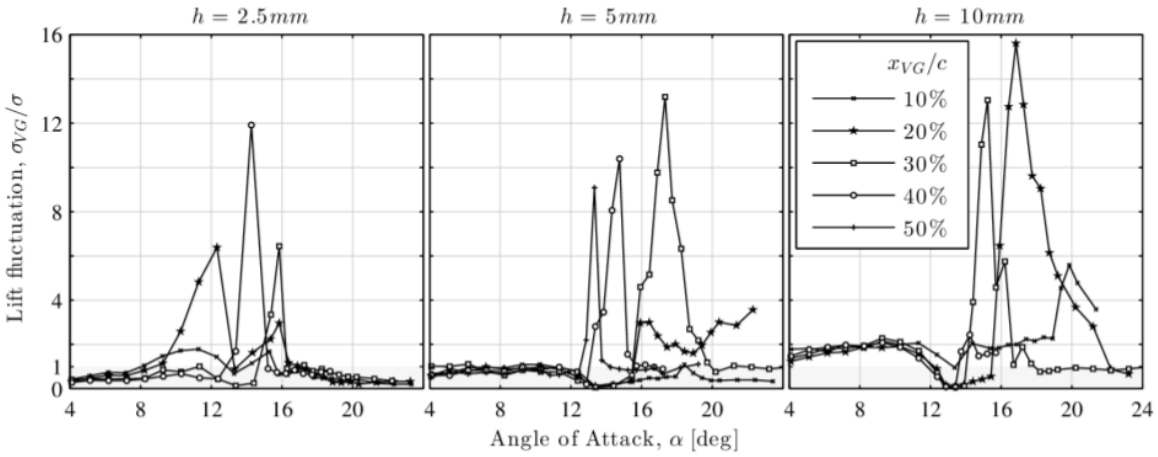

Figure 35 Lift fluctuation for controlled cases relative to the uncontrolled cases

Vortex generator measurements in thickened boundary layers

The wakes of low-profile, rectangular vane-type vortex generators were measured in a thick, turbulent boundary layer. Measurements were conducted in the TU Delft Boundary Layer Wind Tunnel, with corresponding Re_θ≈2200. Particle Image Velocimetry was deployed to provide three-component velocity fields. This allowed assessment of numerous aspects:

- Adverse pressure gradient influence on vortex/boundary layer development
- Influence of vortex asymmetry on the interaction of the vortices with the boundary layer
- Extent and relevance of vortex meandering

The fundamental measurements provided additional validation means for the newly implemented VG model (Figure 36).

Main conclusions and comments may be summarized as follows:

- A growing boundary layer will further immerse a VG, weakening the vortices and increasing the level of meander, leading to quicker dissipation of the vortices.
- Vortex asymmetry does not significantly affect the boundary layer evolution for a non-separating flow (Figure 37). Airfoil measurements (T2.4) suggest an amplification of these small differences in strongly adverse pressure gradients, with possible implications of the level and position of maximum lift.
- Inviscid theory predicts the vortex motion well within the first 50 device heights downstream. The same may be said for asymmetric vortices, however extensions to the original vortex models proposed in the 1950s were necessary (Figure 38). Even for complex turbulent flows such as the one in question, vortex models offer useful physical insights.
- The principal meander motion is directly responsible for distorted vortex shapes observed in the mean flow.
- Vortex meander manifests as apparent stress and added kinetic energy in the mean field statistics. These are the typical means of assessing such flows. Thus, awareness of the meander extent is necessary when benchmarking numerical tools (Figure 39 and Figure 40).

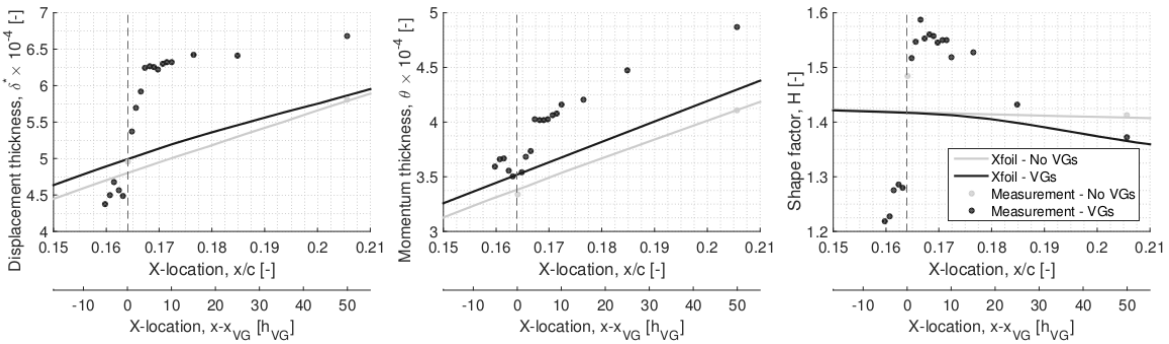

Figure 36 Evolution of IBL parameters: comparison of measurements and model preidctions

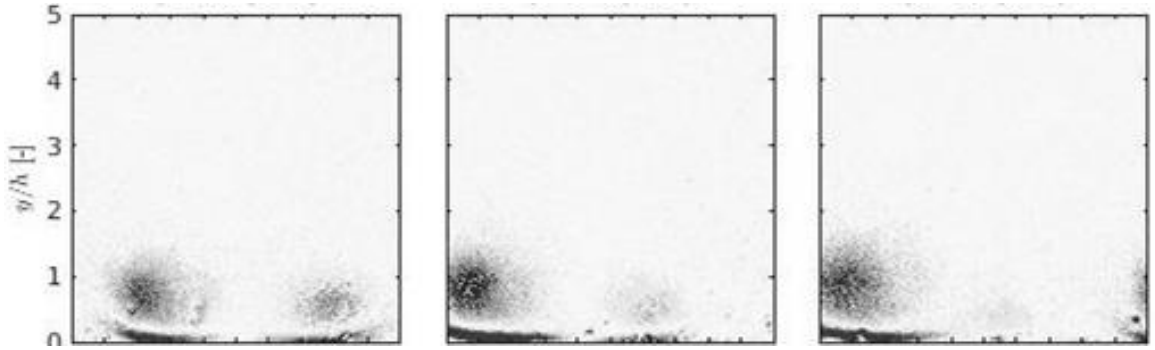

Figure 37 Vortex core vorticity at *10h* downstream for increasing (left to right) vortex asymmetry

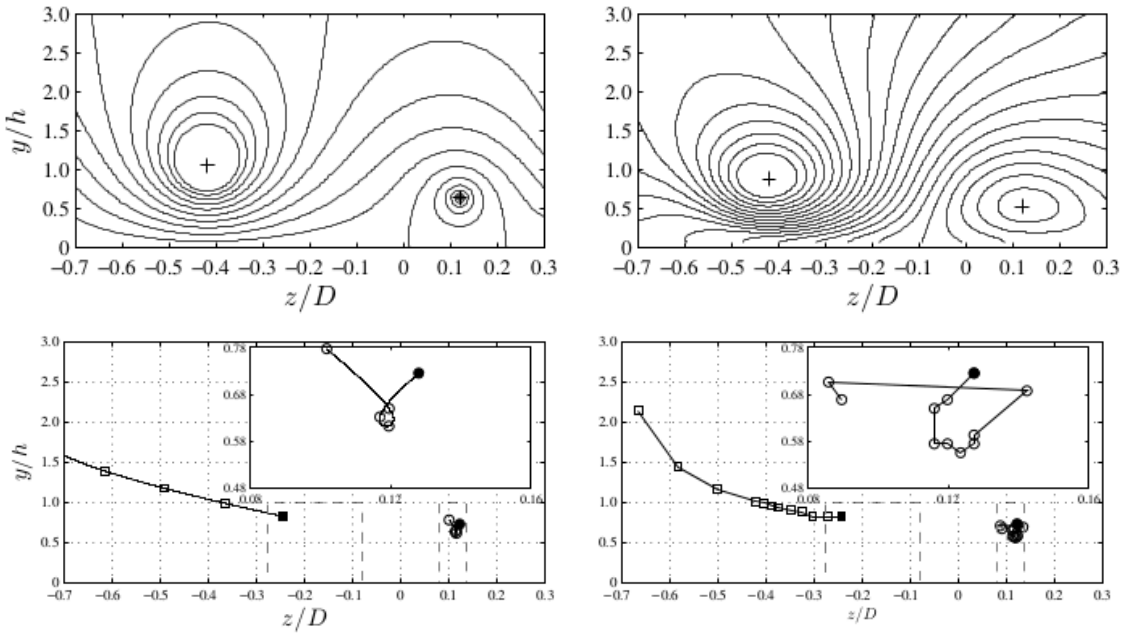

Figure 38 Stream function at 10h downstream (top) and vortex trajectories projected in a frontal plane (bottom). Vortex model (left) and measurements (right)

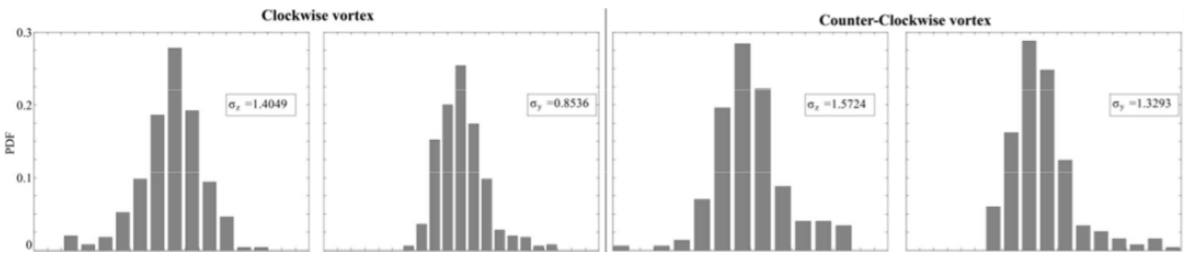

Figure 39 Statistical analysis of the vortex core dynamics

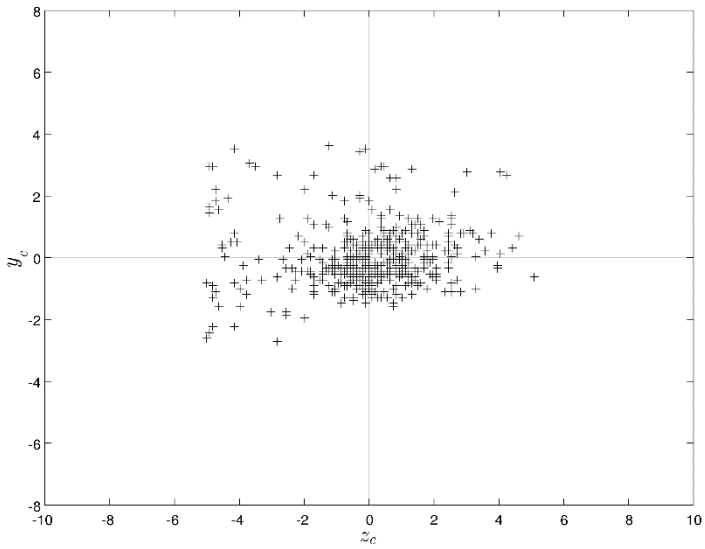

Figure 40 Visual impression of the unsteady nature of the primary vortex

2.3 WP3: Reduction of uncertainties by integral substructure design

Background

The aim of this work package is to investigate where cost reductions in the support structure are possible while keeping a sound and safe design. Probabilistic design methods (structural reliability methods) are used to study whether there is any conservatism in the design of support structures.

At this moment the design of support structures for offshore wind turbines is done in collaboration between the wind turbine manufacture and a specialized engineering company like Ramboll and Van Oord. The support structure consists of a foundation, a sub-structure and a tower. The tower is designed by the wind turbine manufacture, while the foundation and sub-structure are designed by the engineering company. The structural design is verified by applying partial safety factors as prescribed in the standards of DNV-GL. Partial safety factors are applied to compensate for uncertainties in the design process, and improved knowledge may help to reduce these factors and hence contribute to reduction in CoE without compromising the reliability of the design.

Approach

As an alternative to partial safety factors, probabilistic design methods will be applied. In the past probabilistic design methods were already used for wind turbines. For instance in the JOULE-III project PRODETO (PRObabilistic DEsign TOol) [1] the PhD-thesis of Veldkamp [2] and the work by Soerensen [3]. The focus in this work package will be on the support structure while taking the complete offshore wind turbine system in to account.

The application of probabilistic design methods should give insight in the following:

- The safety level of an offshore wind turbine based on partial safety factors as prescribed in the standard;
- The safety level in case the life time of 20 years is increased;
- Identification of the importance of the different load parameters to the safety level.

A general framework for reliability assessment of existing monopile design is defined first. As an introduction, design requirements for offshore wind support structures as recommended in guidelines and standards are briefly explained. Next a general framework for reliability assessment of offshore wind support structures is outlined. Finally, the outlined approach is illustrated using a simple case study.

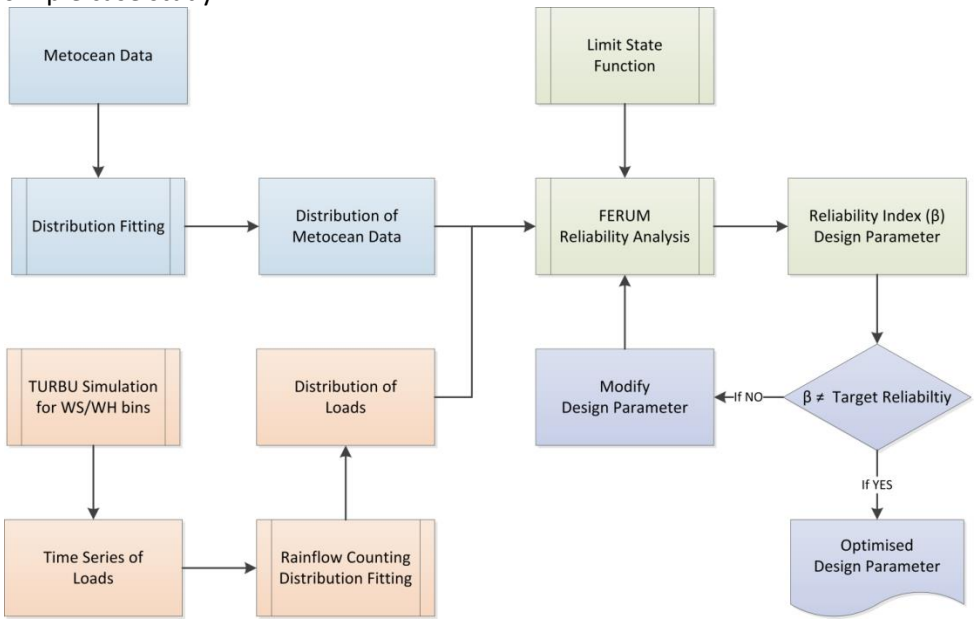

At the start of the project the idea was to adopt the approach of the EU-project Prodeto. In that project first, a database with blade load responses was created both numerical and by measurements. The responses were collected in a scatter diagram (histogram) of the mean wind speed and the turbulence. Finally the statistics of the responses is used as input for the probabilistic design. The disadvantage of this approach is that uncertainty in the input variables cannot be taken into account. For example, the inertia and drag coefficient in the Morison equation calculating the wave load are deterministic. In order to have stochastic input variables, it was decided to generate the database as part of the reliability analysis. During the search for the design point, every change in the input variables means a recalculation of the database (load set).

The recalculation of the data base during the probabilistic analysis puts a constraint on the number of sea state and the selected aeroelastic tool. In the D4rel project the linear code TURBU is used instead of the nonlinear code PHATAS. The metocean climate is described by a different number of sea states:

1. A complete twenty metocean hindcast data set of three hour sea states;
2. A 4D-histogram of binned mean wind speed, significant wave height and peak period;
3. A lumped data set of 12 three-hour sea states.

Both the 4D-histogram and the lumped data set are used during the probabilistic analysis.

As mentioned, a generic probabilistic analysis approach is applied including stochastic input variables where the load set is recalculated in case the input is changed.

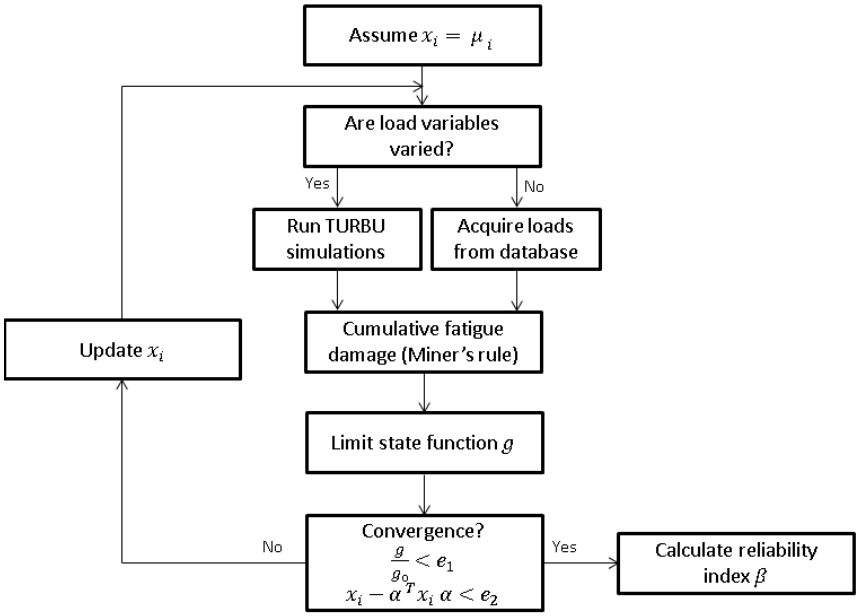

A generic reliability analysis approach is selected. This means that the aeroelastic load calculations are incorporated in the reliability analysis. In the D4rel project, the analysis is performed by coupling the aeroelastic simulation tool TURBU with the open source reliability analysis to FERUM. Different reliability methods are available like the first order and second order reliability method, FORM and SORM, or methods based on Monte Carlo simulations. FORM is used since it calculated the contribution, importance factor, of the stochastic variables to the reliability.

For the probabilistic analysis, a modern 4MW offshore wind turbine is selected. In the probabilistic design approach, the limit state condition is considered. The limit state function g is the difference between the resistance R and the load L. For a safe design the limit function should be larger than zero. In structural reliability, the design point is determined where the limit state function is zero. Three limit state functions are considered:

1. A fatigue limit state;
2. An ultimate limit state on the yield stress;
3. An ultimate limit state on the global buckling stress.

The result of a probabilistic design analysis is a probability of failure and the corresponding reliability index. The calculated failure probability is compared with the probability the monopile is designed for. Industry wants to know how the probability of failure is related to the partial safety factors as prescribed by the design standards. Is the monopile design too conservative? The translation from probability of failure to partial safety factors is not straightforward. First of all in D4rel only a limited number of design load cases are considered compared to the standard. Second, in the standard, one safety factor is given for the strength and one safety factor for the loading dependent on the limit state.

In probabilistic design for every stochastic variable used a partial safety factor can be estimated. The partial safety factor for a variable is defined as the ratio between the value of the stochastic variable at the design point and the so-called characteristic value. In practice, the characteristic value is the 5% quantile for the strength associated variable and for the load associated variable the 98% quantile. The table shows the partial safety factors for the fatigue limit state. The importance factor alpha squared shows the contribution of the variable to the probability of failure. The partial safety factor of log(C1) with the largest contribution is a bit lower than the safety factor in the standard being 1.0.

var	dsptx	char value	PSF	α^2
Strength				
Δ	0.418	1	2.392344	0.1968
log(C1)	12.164	11.764	0.967116	0.0000
log(C2)	14.722	15.606	1.060046	0.7555
Loads				
E	2.10E+11	2.10E+11	1	0.0000
C_D	0.814	0.7	1.162857	0.0383
C_M	2.127	2	1.0635	0.0089
Csoil	5.96E+10	6.60E+10	0.90262	0.0005

Instead of assessing the partial safety factor for an existing design, a monopile can be designed by either using partial safety factors or according to a prescribed probability of failure. In the EU-project Upwind, a cost model was developed where a monopile concept design is generated to estimate the costs. In this cost model, partial safety factors are used. In the D4rel project the cost model is updated using probabilistic design methods. Now for a given probability of failure, the costs of the monopile are estimated.

Results

The final part of the work on structural reliability was the assessment of industry questions. The subject proposed by the industry was a reliability analysis on the soil properties. Based on available literature, it was decided to apply data from Sheringham Shoal [14]. Three different soil layers were considered in the analysis: two clay layers and in between a sand layer. The limit state for the soil conditions is that for given loads the pile head displacement at the mudline should not exceed 0.2m. The pile head displacements are determined by the code called Latpile [15]. In Latpile the p-y curves are calculated.

For a 29m pile penetration the pile design has a small probability of failure. The design seems to be too conservative. Therefore the pile penetration was reduced step by step until the probability of failure was 10e-4. The pile penetration is about 18m then. It should be noted that the penetration depth should be checked on the verticality of the tangent at the pile toe, which is another less strict design requirement.

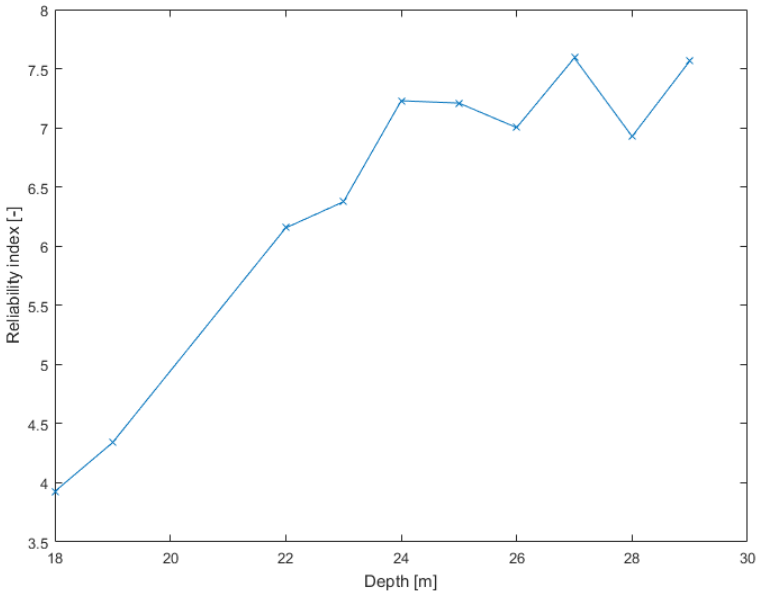

2.4 WP4: System identification for robust control

This section provides a summary of the work performed by TU-Delft in Task 4.1: Non-linear system identification with uncertainty quantification. The work consists of two sub-tasks:

- Task 4.1.1 Uncertainty quantification, and
- Task 4.1.2 Non-linear system identification.

2.4.1 Task 4.1.1 Uncertainty quantification

In Task 4.1.1, it was shown that the uncertainty of identified LPV models can be estimated quantitatively by using bootstrapping techniques. This could potentially lower safety factors and allow less conservative control for higher performance.

The goal is to obtain an algorithm which can quantitatively estimate the uncertainty of LPV models. The purpose of this uncertainty quantification is to reduce conservatism in subsequent control design and structure design. Less conservatism in control design means we can design and safely use more aggressive controllers which squeeze out more performance. For structure design, less conservatism mean lower safety factors and thus leaner designs.

To perform this uncertainty quantification, bootstrapping approaches were used with a single data set. The performance of this uncertainty quantification was evaluated with bootstrapping versus Monte Carlo simulations.

In Figure 41 and Figure 42, a time-varying eigenfrequency is shown for both the estimate and the true values. The reader is referred to deliverable report D4.1.1.2 (see Section 18) for further details.
Additionally, confidence regions are presented, obtained from bootstrapping with a single data set and from Monte Carlo simulations. It is visible that the bootstrap confidence regions are slightly larger than but very comparable to the confidence regions obtained from Monte Carlo simulations.

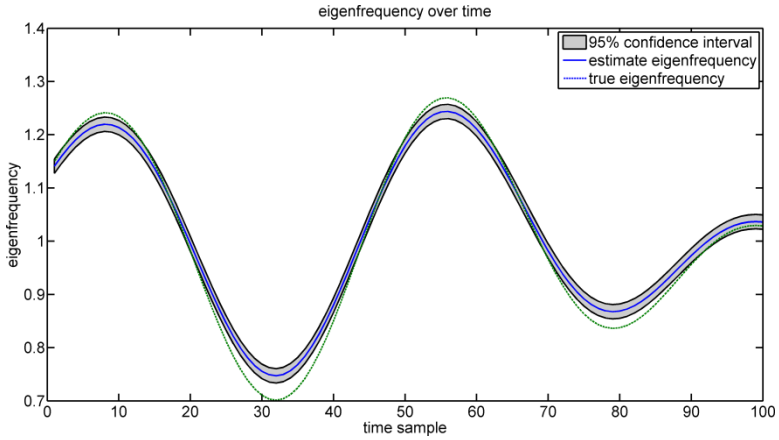

Figure 41 This figure shows both the true and estimated time-varying eigenfrequency. Furthermore in grey are the 95% confidence regions based on bootstrapping results.

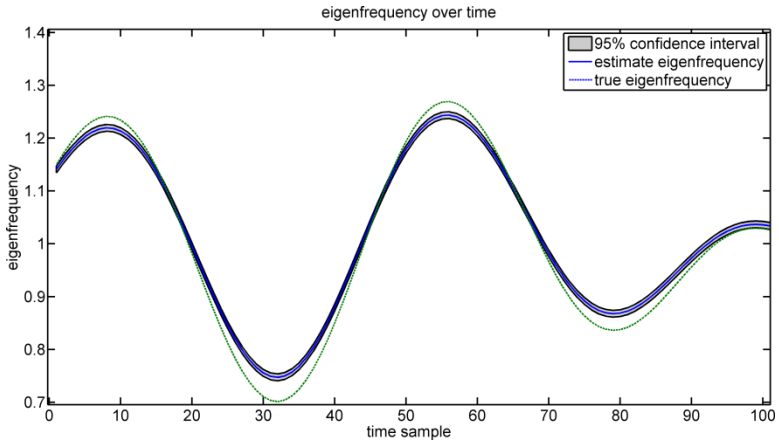

Figure 42 This figure shows both the true and estimated time-varying eigenfrequency. Furthermore in grey are the 95% confidence regions based on Monte Carlo results.

2.4.2 Task 4.1.2 Non-linear system identification

In Task 4.1.2, three “curse-of-dimensionality”-free tensor methods have been developed with improved conditioning for Linear Parameter Varying (LPV) state-space identification. This improved conditioning is due to efficient data use through exploitation of more a priori knowledge, and yields reduced uncertainty sets.

The goal is to develop LPV identification schemes that beat the “curse-of-dimensionality” in state-of-the-art techniques by using tensor algebra. In other words, we want to develop methods with improved conditioning, such that we can use data more efficiently and have reduced uncertainty sets. The purpose of this is to obtain better LPV models, which can then be used to design better LPV controllers to obtain higher performance.

The approach taken is to use tensor techniques to exploit a priori known multi-linear structure of the problem to obtain improved conditioning.
This Task has resulted in three novel identification schemes, each accepted or under review by journals. We refer to [16, 17, 18] for their detailed descriptions and thorough performance evaluations.

Two highlights are mentioned here. The method proposed in [16] is arguably the most structure-exploiting LPV subspace method, as it exploits multi-linear structure. The method proposed in [17] is arguably the most mature LPV state-space refinement method as it provides explicit conditioning guarantees.

2.4.3 Task 4.2.1: Controller re-optimization based on identified models

Background:
Offshore wind turbines operate in harsh, time-varying environmental conditions resulting in significant uncertainties during the design. More specifically, wind turbine manufacturers face the problem that the support structure modal parameters (such as frequency and damping) deviate significantly from their design values. Even more, these parameters also vary with time because of e.g., scour, formation of marine sand dunes and biofouling. As the true support structure frequency is not exactly known in advance, is time-varying and deviates from one turbine in the farm to another, a robust design of the support structure is required to ensure it can withstand the worst-case loading that may occur during its lifetime. Even more, the wind turbine controller, tuned for a wrong support structure frequency, is not only expected to perform sub-optimally but might even increase the loads on the support structure as shown below. This leads to conservative designs of the support structure with increased material costs and questionable reliability.

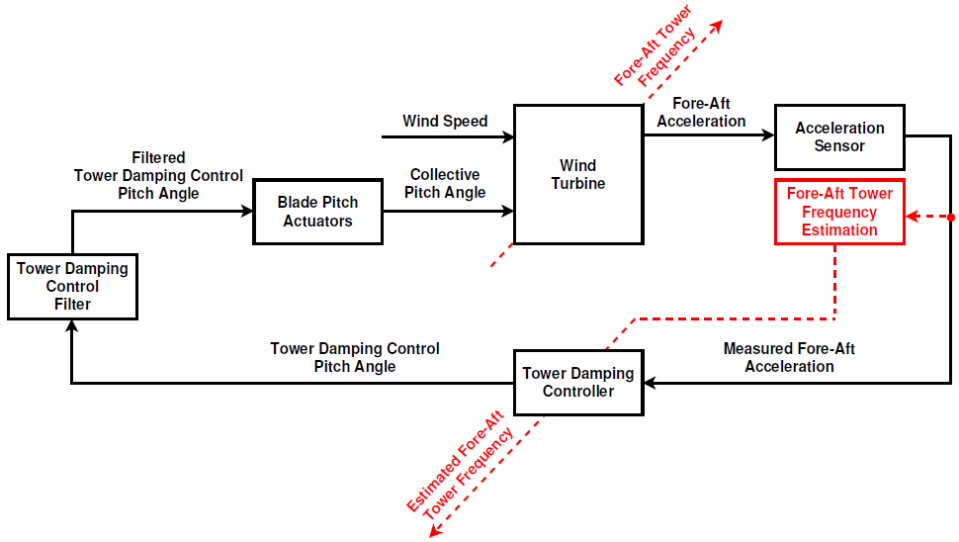

Figure 43 Conceptual view of a nominal tower damping control loop (in black) with the addition of an adaptation mechanism based on the estimated fore-aft tower frequency (in red)

Approach:
In Task 4.2.1 of the D4REL project, an adaptive control algorithm is developed that reduces the loads on the support structure in a worst-case sense in the presence of uncertainty in the support structure frequency. This parameter is assumed to be unknown during the design apart from a realistic possible range of variation, very slowly-varying and online-available (i.e., identifiable using measured data, for one possible approach). Given this setting, the objective is to develop a methodology for the design of a control algorithm that adapts its parameters based on the actually measured, or identified, tower frequency (Figure 43). The purpose is to achieve improved performance in terms of reduction of fatigue loads on the support structure when compared with conventional control where the controller is tuned for the nominal (design) value of the tower frequency. Based on a detailed analysis, the focus of this work is to put on the active fore-aft

tower damping control loop as this loop suffers most by the considered changes in the tower dynamics. Damping of the fore-aft vibrations of the tower is achieved, as usual, by controlling the thrust force on the rotor by means of collectively pitching the blades based on the measured tower top acceleration.

Results

The newly developed adaptive tower damping control is evaluated by means of a comparison to a conventional controller. The study is focused on investigating the DEL reduction potential whenever the first fore-aft natural tower frequency is different from (or changes with respect to) its nominal value. Within the case study, the D4REL wind turbine model is used, representing a generic three-bladed 4 MW wind turbine. The simulations are performed for different wind speeds (partial load and full load). Different values of the tower first natural frequency have been considered, namely the nominal value (0.24Hz), and deviations of approx. 10% (0.21Hz and 0.27Hz) and 20% (0.19Hz and 0.29Hz) from it.

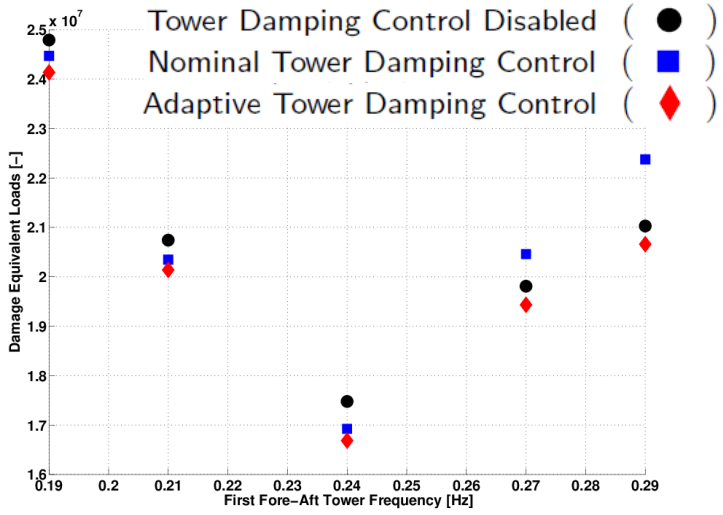

Figure 44 Calculated DELs for partial load conditions

In the simulations, the following controllers are considered:

- Tower damping control disabled
- Nominal Tower Damping Control, tuned based on the nominal first fore-aft natural tower frequency (representing the standard approach to tower damping control)
- Adaptive Tower Damping Control, representing the newly developed adaptive controller that adapts its parameters to the (measured or identified) first fore-aft tower.

In Figure 44 the DELs for partial-load conditions are displayed for the range of investigated fore-aft tower frequencies. As can be seen, both Nominal Tower Damping Control and Adaptive Tower Damping Control both allow for fatigue load reduction when the first fore-aft tower natural frequency is below its nominal value; however, the latter (the new controller) allows for better performance in terms of DELs and reduces by up to 1.5% the worst-case fatigue loads that is obtained by Nominal Tower Damping Control. On the other hand, when the first tower frequency is above its nominal value, the Adaptive Tower Damping Control approach still performs well with respect to the loads obtained by Tower Damping Control Disabled, whereas the Nominal Tower Damping Control approach gives rise to 6.5% higher fatigue loads.

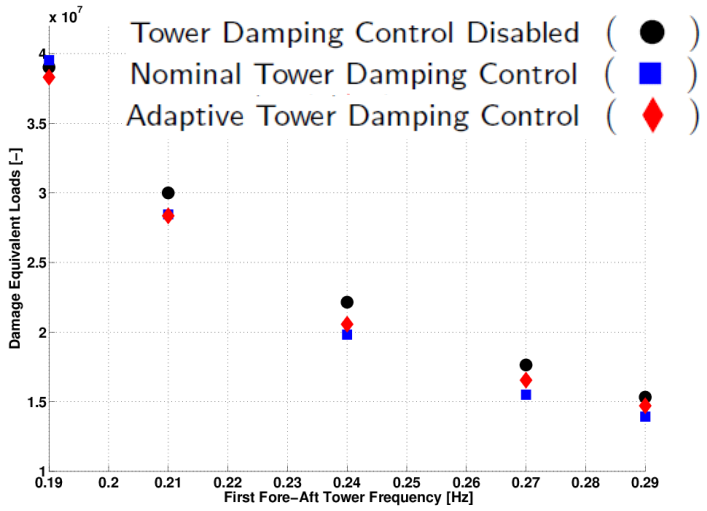

Figure 45 Calculated DELs for full load conditions

In terms of full-load performance, as shown in Figure 45, the Adaptive Tower Damping Control approach performs well for the entire range of investigated fore-aft natural tower frequencies and reduces the fatigue loads by up to 7% compared to the open-loop fatigue loads. As a general trend, for tower frequencies above the nominal value this control strategy is outperformed by the Nominal Tower Damping. However, the highest loads are incurred when the tower frequency is below its nominal value (at 0.19Hz), in which case the new is advantageous achieving lower DEL on the tower. In this case, the newly developed Adaptive Tower Damping Control strategy reduces the fatigue load by as much as 3%.

Summary:
The study has revealed that the current approach to tower damping control does not provide optimal fatigue load reduction performance when the natural tower frequency of the wind turbine is different from its nominal value, typically used for the design of the controller: whereas in some situations the DEL reduction is less significant than in the nominal case, several scenarios have shown that such an approach could even increase DELs when compared with open-loop operation. On the other hand, the proposed adaptive tower control strategy has been shown to bring guaranteed and satisfactory performance in almost all situations. Based on a case study, this strategy shown to achieve a reduction of fatigue loads on the support structure of up to 3%. For the support structure, reduction of fatigue load is commonly considered to enable material cost saving of the same order, which indicates that the proposed adaptive control algorithm can achieve a significant cost savings.

2.4.4 Task 4.2.2: Controller reconfiguration for degraded wind turbine components

Background
Offshore wind farms are expensive to maintain and it is difficult to achieve a similar availability to onshore farms. In D4REL, the possible benefit of condition based control is examined, where the controller is adapted to modify the loading of parts depending on their condition. This benefit is only examined in terms of annual electricity production. Other, secondary benefits may be possible, but are not considered.

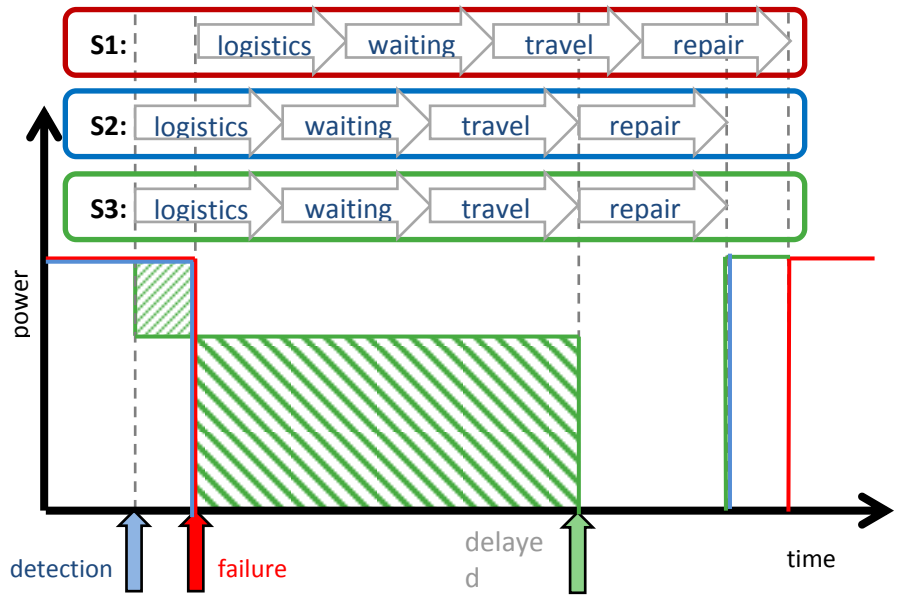

Figure 46 Different O&M scenarios considered

To be able to judge the value of condition based control, three different O&M scenarios are considered as illustrated in Figure 46:

- Scenario 1 Repair on failure: In this scenario, the wind farm operator is only able to detect what failure occurred, after the fact. Up to the moment of the failure, the wind turbine runs at full power. Only after the moment of failure, a repair is planned and executed. After the repair, the turbine starts running at full power again (weather permitting).
- Scenario 2 Condition based maintenance: The presence of a condition monitoring system allows the operator to start planning a repair before the failure actually occurs. Otherwise no action is taken and the turbine remains running at full power until failure occurs. Down time can be reduced by the time between detection and repair, power production increases accordingly.
- Scenario 3 Condition based control: After detection, the turbine is instructed to use reduced operation to delay the failure. Ideally, failure is delayed up until the point of repair. That means that power is lost between the point of detection and the point of (undelayed) failure, but the wind turbine can still generate power after that point, because the failure of the part is delayed. Ideally, this reduced production could be maintained up until the point of repair.

Figure 46 shows that for condition based control to be worthwhile, the power produced after the expected point of failure, must exceed the loss in power production up to the point of failure (the hatched areas respectively to the right and the left of the normal failure point).

Condition based maintenance

First, a literature study was performed on condition monitoring and condition based maintenance (CBM). It indicated that the most relevant parts are the drive train, the blades and the pitch systems. Literature does not give a clear relation between loading and remaining life time of the components, so it is assumed that the remaining life time is inversely related to the loading of the parts.

Next, the study outlined the results of the Baseline O&M strategy and the comparison with two alternative cases whereby CBM is employed:

- CBM is employed for 50% of maintenance activities (CBM 50%)
- CBM is employed for all of the maintenance activities (CBM 100%)

For clarity in the comparison of the modelled O&M strategies in this section, the following points outline the assumptions and logic employed in this subsection:

- The increase in lifetime of components through active load management cannot be quantified, as such, failure rate of components is kept constant in both cases. This may lead to under prediction of cost savings as damage and failures can propagate to cause higher failure rates in other components.
- Furthermore, the ability to derate a turbine for condition based monitoring strategies is not included in the model. This is considered in the section which follows.
- There is no ability to postpone corrective maintenance that long as to allow for performing preventative maintenance. This is both unrealistic and difficult to model. Therefore, the study accepts maintenance costs stay equal. CoE reductions are solely achieved through reduced downtime of the plant.

Based on the aspects positively and negatively affecting the cost of energy in the O&M tool modelling, it can be concluded that the CBM strategy with 100% CBM for small and large components gives a reasonable estimate as to the maximum benefit that results from the proposed condition monitoring combined with load management. This will obviously differ for other wind farms with larger logistic and travel times.

An overview of the results of the modelling of the three O&M strategies is presented in Table 4. Two of the predictions outlined in the points above are immediately notable:

- Cost of repair for all three strategies is equal
- The cost saving benefit is directly proportional to the amount of corrective or condition based maintenance that is employed.

	Baseline	CBM (100%)	CBM (50%)
Availability [%-time]	92.6%	94.3%	93.4%
Availability [%-energy]	91.9%	93.9%	92.9%
Revenue losses [M€/year]	14.9	11.3	13.1
Costs of repair [M€/year]	48.0	48.0	48.0
Costs [€ct/kWh]	3.69	3.61	3.65
Total effort [M€/year]	62.9	59.3	61.1
Energy Production [MWhr/year]	1,302,133	1,329,994	1,316,064
Energy Benefit [MWhr/year]	-	27,861	13,931
Cost Benefit [M€/year]	-	3.6	1.8

Table 4 Comparison of several O&M strategies

The benefits from implementing CBM are indeed notable. Availability of the plant increases 1.7% and 2.0% in terms of time and energy yield respectively. The increased availability of the plant results in a 3.6 M€/year reduction in overall cost of the plant attributed solely due to increased energy yield due to minimized downtime representing the best case scenario. For the CBM 50% strategy, the benefit is half that of the CBM 100% one.

For the considered reference wind farm (consisting of 120 3MW wind turbines), this boils down to 72 M€ over the lifetime of the farm. However, this figure represents an upper limit on the achievable benefit as it is based on an idealistic scenario. More specifically, it is computed by assuming that CBM is applied to all turbine components and that the condition signal is always received enough in advance of the actual failure to allow for performing the O&M planning and waiting activities before the actual failure occurs. The calculation of a more accurate estimate of

the achievable benefit requires more detailed data on the failure prediction capabilities of the condition monitoring systems, which was not available in this study. However, if for example CBM is applied to only 50% of the cases, and if the assumed percentage of the logistics/waiting time that the turbine remains in operation is reduced from 100% to 30%, the lifetime revenue increase would drop down to the more realistic value of 10.8 M€ (availability increase by 0.3%).

Condition based control

Condition based control aims to reduce turbine downtime by taking off the loads from deteriorated components. The load reduction is achieved by operating (controlling) the turbine in a specific way, and is meant to reduce the chances of occurrence of an approaching failure, thereby delaying the failure (Figure 46). To this end, control strategies are investigated that can reduce the loading on specific components of the wind turbine, while at the same time keeping the wind turbine running and not increasing loads on other parts of the wind turbine excessively.

As mentioned before, the focus of this study is to examine strategies for use in case of a worsening condition and approaching failure of particular parts. Two different concepts are examined:

1. Several strategies for power down-regulation. These have the advantage that they may already be available in the existing controllers for grid support functions
2. A novel pitch actuator duty reduction strategy

Condition based control by power down-regulation

Several down-regulation strategies are derived from the nominal control strategy. Roughly speaking, a wind turbine has two different operational regions. The first region consists of operation below the rated wind speed and is referred to as partial load. The second region is called full load and consists of wind turbine operation above rated wind speed. Down-regulation strategies for both regions are discussed and their effects on the loads on different components are studied.

In partial load, three different power down-regulation strategies are considered (see Figure 47):

- Strategy 1: reduction of the tip speed ratio (TSR) at constant pitch angle θ, until stall is approached, after which pitch angle θ increases to stay away from stall
- Strategy 2: TSR is increased, while at the same time slightly modifying the pitch angle θ to ensure we remain at the right slope of the power curve
- Strategy 3: pitch angle θ is increased, keeping the TSR constant.

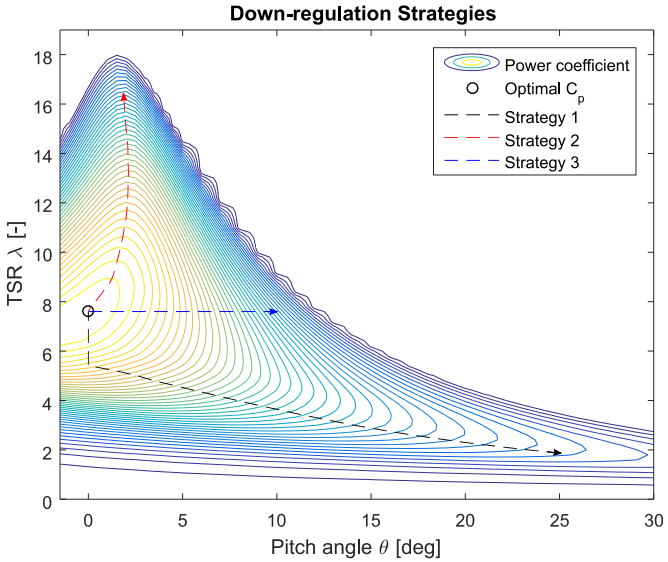

Figure 47 Contour plot of a wind turbine's power coefficient data indication three down-regulation strategies in partial load

In full load, the wind turbine operates at the rated generator torque τ_g and the rotor is controlled at its rated value through a pitch action of the blades. In the case of down-regulation at full load, two methods are considered. The first method is called de-rating and consists of decreasing the rated generator torque τ_g by a desired percentage. The second method reduces the rated generator speed Ω_g by the desire percentage.

Table 5 gives an overview of the total of six strategies considered.

Strategy	Partial Load	Full Load
1a	$TSR\searrow, \theta\nearrow$	$\tau_g\searrow$
1b	$TSR\searrow, \theta\nearrow$	$\Omega_g\searrow$
2a	$TSR\nearrow, \theta\nearrow$	$\tau_g\searrow$
2b	$TSR\nearrow, \theta\nearrow$	$\Omega_g\searrow$
3a	$\theta\nearrow$	$\tau_g\searrow$
3b	$\theta\nearrow$	$\Omega_g\searrow$

Table 5 Overview of the studied down-regulation control strategies

In order to test the performance of the different controllers in terms of their load reducing capabilities, they are used in the aeroelastic simulation tool PHATAS. A desired down-regulation percentage of 20% is selected in the case study. Since the effect on fatigue loads are of primary interest, simulations are performed for normal operation with turbulent wind speeds ranging from 4-25 m/s with six realization per wind speed.

The performances of the down-regulation strategies are subsequently compared to the case of the baseline controller in terms of Damage Equivalent Loads (DELs) on a number of selected structural wind turbine components, i.e., the tower (bottom), the blade roots, the rotor shaft and yaw gearbox. It has to be noted that the results for each part are given in the resultant direction. For the tower this means that DELs of the combined motion in the Fore-Aft and Side-Side direction are computed. Finally, the lifetime loads are calculated and summarized in Table 6.

	Strategy 1a	Strategy 1b	Strategy 2a	Strategy 2b	Strategy 3a	Strategy 3b
Tower bottom	+1.8%	-0.2%	-17.6%	-12.7%	-13.2%	-9.1%
Blade roots	-8.9%	-25.1%	-14.6%	-24.0%	-14.2%	-24.8%
Rotor shaft	-4.9%	-17.9%	-0.9%	-14.2%	-4.2%	-15.9%
Rotor Tilt	-5.4%	-18.3%	-0.9%	-14.4%	-4.7%	-16.2%
Rotor Yaw	-5.5%	-17.3%	-1.3%	-13.8%	-4.8%	-15.4%
Energy production	-17.1%	-20.1%	-20.8%	-20.3%	-20.3%	-20.7%

Table 6 DELs of several structural wind turbine components relative to the performance of the baseline controller

The presented loads analysis indicates that the investigated down-regulation strategies generally reduce the fatigue loading on the turbine components. For condition based control, the most beneficial strategy depends on the deteriorated component that needs to be operated at reduced loading. From Table 6, it becomes clear that strategy 1b (operation at reduced TSR in partial load, and reduced rated rotor speed in full load) has most pronounce impact on the lifetime loads on

most components, which suggests that strategy to be the first choice. However, a closer analysis [19] indicates that for wind speeds below rated the tower loads may increase substantially, and therefore depending on the current wind conditions this strategy may not be desirable. In partial load, strategy 2b has higher tower load reduction potential, but the loads on blades and shaft are worse. Therefore, the strategy selection depends on the component of interest and the wind conditions.

The following components were identified to have high potential for achieving economic benefits when condition based maintenance and control is applied to them (see [19] for details):

- **Generator**: with respect to the generator, down-regulation in combination with a lower electric torque seems the most suitable strategy. This corresponds to **Strategy 1a** (operating at decreased tip speed ratio [and lower torque] below rated, and reduced rated torque above rated). This strategy may increase tower loads at below rated wind conditions somewhat, but the other loads remain lower.
- **Gearbox**: all strategies involving reduction of the rated rotor speed (Strategies 1b, 2b and 3b) in full load result in lower loads on the shaft. In partial load, however, 2b does not perform well as it increases the loads on the shaft for some wind speeds. **Strategy 1b**, or alternatively 3b, are preferable with respect to the reduction of loads on the gearbox. If the largest possible load reduction is aimed (especially in partial load), then strategy 1b should be used. Between 8 and 10 m/s, the load reduction is around 30%. However, if the loads on the remaining components is considered important as well (and particularly the tower loads), **Strategy 3b** becomes the best option.
- **Yaw gearbox**: from the components analyzed, the rotor yaw moment is most closely related to the load on the yaw gearbox. Similar discussion hold here as for the gearbox, suggesting **Strategy 3b** as preferred option.
- **Pitch mechanism**: all power down-regulation strategies, considered in this section increase the pitch actuator duty cycle because the rotor speed control by blade pitching starts at lower wind speeds compared to the normal operation. Loads on the pitch mechanism can be reduced using another control strategy, discussed in the next section.

Condition based control for the pitch mechanism

Down-regulation control strategies were argued above to be beneficial for condition based control with respect to some of the turbine components, namely the generator, the gearbox and the yaw gearbox. However, these were argued to have a negative (undesired) impact on the pitch duty cycle as the blades start pitching at lower winds to derate the turbine. Therefore, an alternative approach for condition based control is developed that targets the pitch systems specifically. The pitch system is important to consider with condition based control as it causes the highest number of incidents and significant down time.

The idea is to reduce the pitch activity by using the generator torque to assist the pitch control loop in controlling the rotor speed. The generator torque is only allowed to vary up to some maximum allowed torque and the rotor speed is allowed to vary in a margin around the rated rotor speed. Once the rotor speed exceeds this margin, pitch is used to return the rotor speed to within the assigned rotor speed margin, after which the generator torque control takes over the rotor speed regulation again.

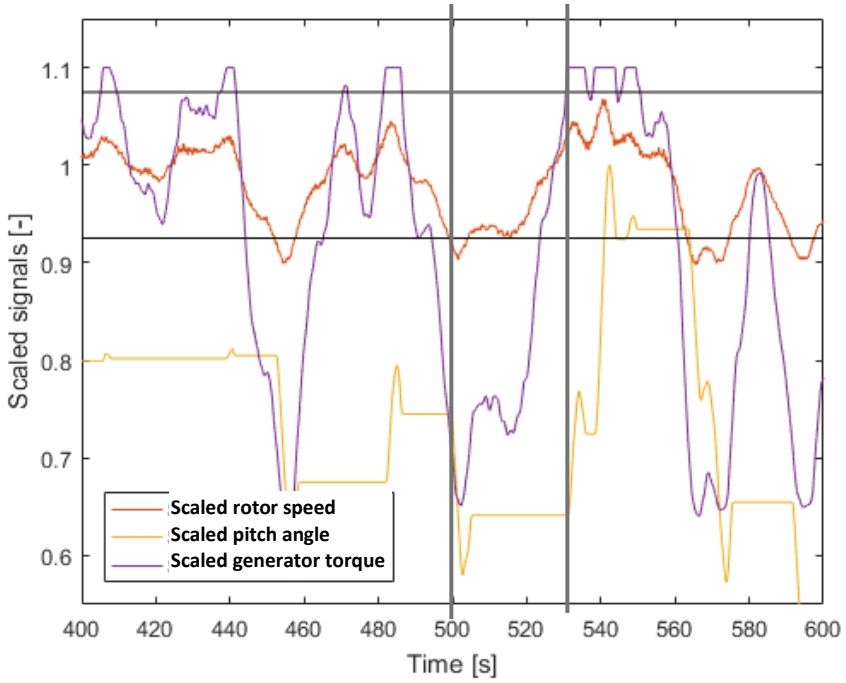

Figure 48 Reduced pitch algorithm behavior

Figure 48 shows the behavior of the reduced pitch algorithm using scaled pitch angle, generator torque and rotor speed signals (all normalized). As mentioned, the rotor speed is controlled with the torque within a predefined rotor range. Pitching is reduced to the moments when the rotor speed leaves this range or when the generator torque reaches its maximum torque. For instance, just before the 500 seconds into the simulation, the rotor speed drops below rated rotor speed – 1 rpm, and the controller reduced the pitch angle. Pitching stops once the rotor speed has recovered sufficiently. Just after 530 s, the rotor speed is increasing above rated and now the torque hits its maximum value. Pitching starts once the maximum generator torque is achieved and stops once the rotor speed is at the same value at which maximum torque was achieved.
Simulations were run with the generator torque allowed to vary up to 10% above rated torque. The margin on the change of the rotor speed at which pitch control takes over is varied from 0.2 rpm to 1.0 rpm to study its effect on the achievable performance.

Table 7 and Table 8 show the results in terms of fatigue load and duty cycle reduction. The simulations show that targeting the pitch effort with this specific strategy results in an average 54% reduction of the pitch effort at the cost of 7% reduction in power production. That means that a 7% reduction in produced power can be used to achieve a doubling in the remaining time until failure and thus up to 102% ((100%-7%)/46%) increase in overall energy production.

	Reduced pitch Strategy
Rotor – flapwise	0.9579
Rotor – leadwise	1.0044
torque on drive train support	1.1532
Main shaft - yaw loading	0.9951
Main shaft – tilt loading	0.9858
Tower – fore aft	0.9672
Tower – side to side	0.9765

Table 7 Reduced pitch in full load: fatigue loads (Weibull weighted)

	Reduced pitch strategy
Generator	1.00
Pitch activity	0.46

Table 8 Reduced pitch in full load: generator and pitch activity, wind speeds 14-25 m/s

It should also be noted that it is possible to combine the pitch control strategy with one of the other power reducing strategies to give sufficient headroom in terms of maximum torque, power or rotor speed. This particular condition control strategy comes at the expense of larger power fluctuations in full load and requires some margin in terms of maximum torque and power relative to rated conditions. Furthermore, the loads on the main shaft increase somewhat due to the increased torque actuation (see Table 7).

Benefits:
Here, the estimated economic benefits are summarized. For the underlying analysis, please refer to [19].

With respect to condition based control, two methods have been investigated: power down-regulation and a novel pitch reduction control. Both methods deliver fatigue load reductions at the expense of some power loss, but are complementary as they target different components. In terms of economic benefits, significant revenue improvements are estimated by combining condition monitoring systems with CBM and condition based control, ranging from 1.5-1.7 M€ (for the gearbox and the yaw mechanism) to 2.7 M€ (for the pitch system). This sums up to a total of 5.9 M€ additional revenue. This benefit is solely due to an increased availability by 0.17%. This benefit comes in addition to those from CBM, so that a total of 0.47% increase in availability is obtained.

3. Impact

In this section, the contributions of the D4REL project to the objectives in the TKI Wind op Zee programme are discussed. More specifically, the cost reduction of the offshore wind energy objective is targeted with this project.

In the project plan, an ambitious quantitative estimation was made for the achievable cost savings aimed with this project. At the project end, a detailed quantitative analysis of the CoE is performed and reported in project deliverable D4.3 [20]. Here, the CoE analysis results are only summarized (see Table 9), for details regarding the cost modeling approach and the assumptions made please refer to [20].

Cost component	CAPEX		OPEX	AEP	
Technology	Blades	Support structure	O&M	Gross AEP	Availability
Generator modularity					0.06%
Termal management					0.02%
Vortex generators				2%	
Thick trailing edges		0%		0%	
Probalistic design		6.7%			
Adaptive control		3%			
Condition based control					0.47%
Total		9.7%		2%	0.55%

Table 9 Quantitative analysis of the impact of the D4REL technologies on the CoE

It is interesting to note that the quantitative CoE analysis indicated a higher overall benefit that estimated at the beginning of the project.

The overall effect shown is:

- on AEP: approximately is 2.5% , based on 2% increase in AEP due to vortex generators and approximately 0.5% increase in availability.

- 9.7% reduction of the support structure CAPEX. The share of the support structure cost on the total required CAPEX of an offshore wind farm is approximately 20 – 25%, for water depth of approximately 30 – 35 m. This would then result in a total reduction of CAPEX of approximately 2%.

ECNs cost model shows that for large offshore wind turbines the LCoE is based on 55 – 65% on the capital cost and for 35 – 45% on the operational cost. Applying these shares the total cost reduction due to D4Rel investigated innovations can be 1-(1-0.6*0.02)/1.025 resulting in approximately 3.6% cost reduction of the LCoE.

In the project plan, the expected impact was estimated at a total of 6% reduction of CAPEX, 4% reduction of OPEX, and 1.25% AEP increase. The total LCoE reduction target, set at the proposal stage, 1-(1-0.6*0.06-0.4*0.04)/1.0125=6.4%, proves to have been quite ambitious.

References

[1] H. Braam, „Probabilistic design tool PRODETO: Final report EU JOULE III project JOR3-CT95-0026," ECN, report ECN-CX—99-046, Petten, Netherlands, 1999.

[2] H. Veldkamp, *Chances in wind energy: A probabilistic approach to wind turbine fatigue design,* Delft: TU-Delft, 2006.

[3] J. Soerensen, „Reliability-based calibration of fatigue safety factors for offshore wind turbines," *International journal of offshore and polar engineering, 22(3),* 2012.

[4] v. d. Veen, *Identification of Wind Energy Systems,* TU-Delft, 2013.

[5] J. v. Wingerden, „The Asymptotic Variance of the PBSIDopt Algorithm," in *Proceedings of the 16th IFAC conference on system identification (SYSID 2012)*, Brussels, Belgium, 2012.

[6] J. Carroll, A. McDonald en D. McMillan, „Reliability comparison of wind turbines with dfig and pmg drive trains," *IEEE Transactions on Energy Conversion,* vol. 30(2), p. 663–670, 2015.

[7] R. Bayerer, T. Herrmann, T. Licht, J. Lutz en M. Feller, „Model for Power Cycling lifetime of IGBT Modules," *Integrated Power Systems (CIPS),* pp. 1-6, 2008.

[8] P. Fuglsang, I. Antoniou, K. Dahl en H. A. Madsen, „Wind tunnel tests of the ffa-w3-241, ffa-w3-301 and naca 63-430 airfoils," Risoe, Report number Risoe-R; No. 1041(EN), 1998.

[9] D. Baldacchino, D. S. Ragni, C. Ferreira en G. v. Bussel, „Towards integral boundary layer modelling of vane-type vortex generators," in *Proceedings of the AIAA, June 2015*.

[10] C. Velte, V. Okulov en I. Naumov, „Regimes of flow past a vortex generator," *Technical Physics Letters,* vol. 38, nr. 4, pp. 379-382, 2012.

[11] T. Doligaslki, C. Smith en J. Walker, „Vortex interactions with walls," *Annu. Rev. Fluid. Mech,* vol. 24, pp. 573-616, 1994.

[12] [Online]. Available: http://www.lr.tudelft.nl/organisatie/afdelingen/aerodynamics-wind-energy-flight-performance-andpropulsion/.

[13] W. Timmer en R. van Rooij, „Summary of the Delft University Wind Turbine Dedicated Airfoils," in *AIAA-2003-0352*, 2003.

[14] T. M. H. Le, G. R. Eiksund, P. J. Strøm en M. Saue, „Geological and geotechnical characterisation for offshore wind turbine foundations: A case study of the Sheringham Shoal wind farm," *Engineering Geology,* vol. 177, pp. 40 - 53, 2014.

[15] *LatPilePY v1.04,* Interactive Design Services Pty Ltd, 2012.

[16] B. Gunes, J.-W. v. Wingerden en M. Verhaegen, „Predictor-based tensor regression (PBTR) for LPV subspace identification," *Automatica,* vol. 79, pp. 235 - 243, 2017.

[17] B. Gunes, J.-W. v. Wingerden en M. Verhaegen, „Tensor networks for MIMO LPV system identification," *in preparation 2017.*

[18] B. Gunes, J.-W. v. Wingerden en M. Verhaegen, „Tensor nuclear norm LPV subspace identification," *submitted to Transactions on Automatic Control ,* 2016.

[19] W. Engels, A. Marina, S. Kanev en D. v. d. Hoek, „Condition based control," ECN, D4REL deliverable D4.2.2., September 2017.

[20] S. Kanev en B. Bulder, „Integral impact of the results from D4REL on the cost of energy at system level," ECN, D4REL deliverable D4.3, September 2017.

[21] J. v. Wingerden en M. Verhaegen, „Subspace identification of Bilinear and LPV systems for open and closed loop data," *Automatica, 45(2),* pp. 372-381, 2009.

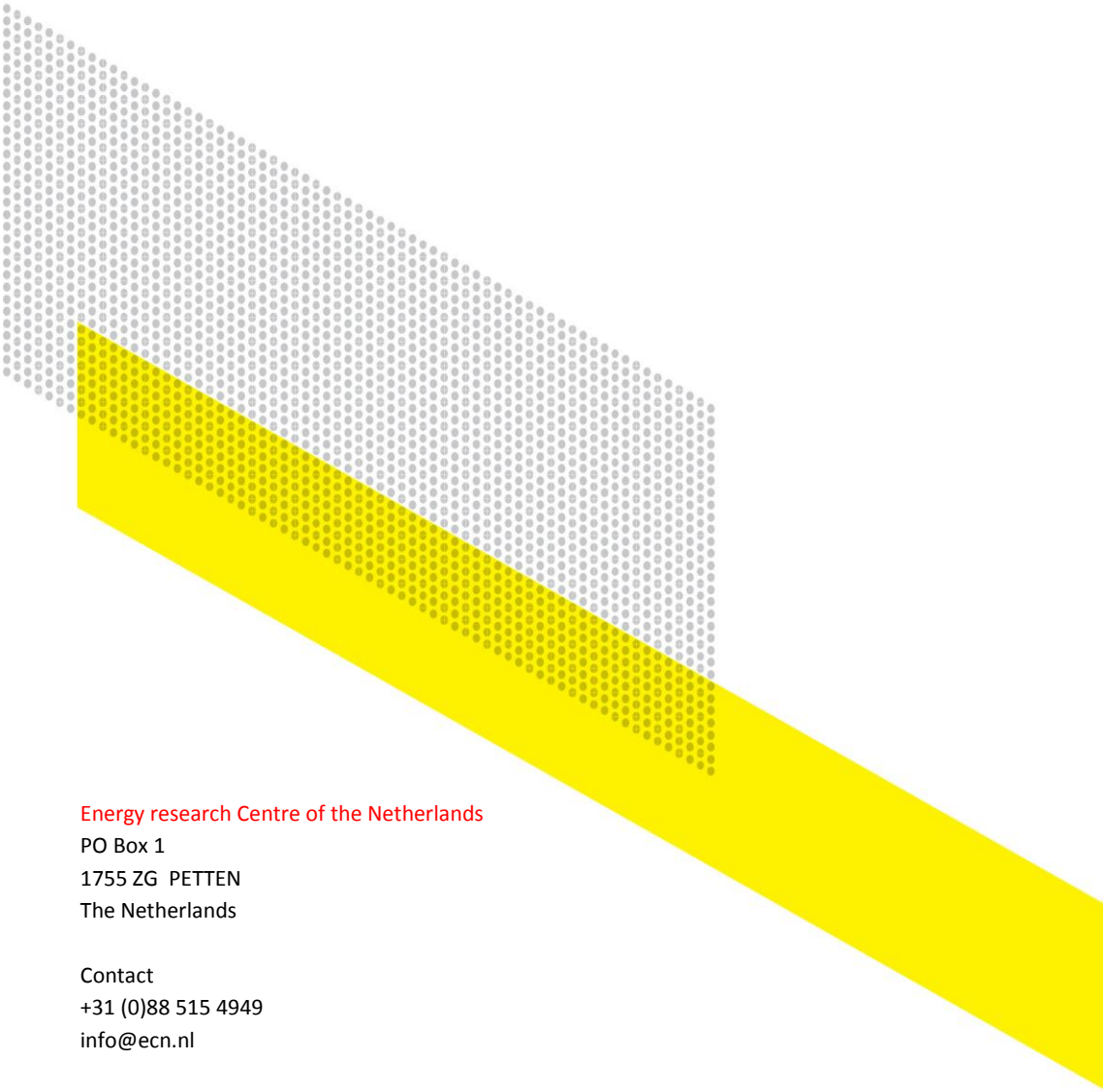

Energy research Centre of the Netherlands
PO Box 1
1755 ZG PETTEN
The Netherlands

Contact
+31 (0)88 515 4949
info@ecn.nl

www.ecn.nl